1370 J. Med. Chem. 2010, 53, 1370–1382
DOI: 10.1021/jm9016703

Journal of Medicinal Chemistry Article

Conjugates of Desferrioxamine B (DFOB) with Derivatives of Adamantane or with Orally Available Chelators as Potential Agents for Treating Iron Overload

Joe Liu,[†] Daniel Obando,[†] Liam G. Schipanski,[†] Ludwig K. Groebler,[‡] Paul K. Witting,[‡] Danuta S. Kalinowski,[‡] Des R. Richardson,[‡] and Rachel Codd*,[†]

[†]*School of Medical Sciences (Pharmacology) and Bosch Institute, University of Sydney, New South Wales 2006, Australia and* [‡]*School of Medical Sciences (Pathology) and Bosch Institute, University of Sydney, New South Wales 2006, Australia*

Received November 12, 2009

Desferrioxamine B (DFOB) conjugates with adamantane-1-carboxylic acid, 3-hydroxyadamantane-1-carboxylic acid, 3,5-dimethyladamantane-1-carboxylic acid, adamantane-1-acetic acid, 4-methylphenoxyacetic acid, 3-hydroxy-2-methyl-4-oxo-1-pyridineacetic acid (*N*-acetic acid derivative of deferiprone), or 4-[3,5-bis(2-hydroxyphenyl)-1,2,4-triazol-1-yl]benzoic acid (deferasirox) were prepared and the integrity of Fe(III) binding of the compounds was established from electrospray ionization mass spectrometry and RP-HPLC measurements. The extent of intracellular ^{59}Fe mobilized by the DFOB-3,5-dimethyladamantane-1-carboxylic acid adduct was 3-fold greater than DFOB alone, and the IC_{50} value of this adduct was 6- or 15-fold greater than DFOB in two different cell types. The relationship between log*P* and ^{59}Fe mobilization for the DFOB conjugates showed that maximal mobilization of intracellular ^{59}Fe occurred at a log*P* value ~2.3. This parameter, rather than the affinity for Fe(III), appears to influence the extent of intracellular ^{59}Fe mobilization. The low toxicity-high Fe mobilization efficacy of selected adamantane-based DFOB conjugates underscores the potential of these compounds to treat iron overload disease in patients with transfusional-dependent disorders such as β-thalassemia.

Introduction

Inheritable disorders of hemoglobin arising from monogenic defects are the most common diseases in the world, with about 7% of people estimated as carriers.[1,2] Each year, 300000−500000 children are born with severe hemoglobin disorders, which include sickle cell anemia and the thalassemias.[1] Without treatment for their anemia, these infants die in the first few years of life.[1] Patients with severe forms of β-thalassemia require lifelong blood transfusions at 2−4 weekly intervals.[3] These regular blood transfusions increase macrophage-induced heme catabolism, which releases iron into the serum. This saturates the iron transport protein, transferrin, resulting in an increased pool of nontransferrin-bound-iron (NTBI[a]).[4] Humans do not have an active iron excretion mechanism, and levels of NTBI in excess of the normal, tightly regulated Fe(III) concentrations (about 10^{-24} M) can generate reactive oxygen species (ROS) that can cause dysfunction of the heart, liver, anterior pituitary, and pancreas.[5] Therefore, β-thalassemia patients must undergo, in addition to their blood transfusions, treatment with chelating agents that coordinate the excess iron and form complexes that are excreted via the urinary and/or fecal route.[6,7] Before the advent of chelation therapy in 1962, β-thalassemia patients maintained on prophylactic blood transfusions would die in early adulthood from complications arising from iron overload.[3]

The first-line treatment for iron overload is the mesylate salt of the trihydroxamic acid-based siderophore, desferrioxamine B (DFOB; **1**), produced by the bacterium *Streptomyces pilosus* (Figure 1).[8] Siderophores are low-molecular-weight organic compounds produced by nonpathogenic and pathogenic bacteria in response to Fe deprivation.[9−12] With poor gastrointestinal absorption and a short plasma half-life ($t_{1/2}$ ~ 12 min),[13] DFOB·mesylate is not orally active, which requires that patients are treated via subcutaneous or intravenous infusion for about 60 h per week.[3] This arduous treatment regimen has a negative impact upon the quality of life of patients. Poor compliance with chelation therapy can lead to siderotic cardiac disease, which accounts for 71% of the mortality from thalassemia.[5,14] Significant drawbacks in the efficacy of the monocationic, hydrophilic **1** (water solubility ~ 0.4 M) as a chelation agent, include both its rapid clearance (reflected in the treatment regimen) and its inability to readily cross cell membranes to access intracellular iron pools.[15] The distinguishing attribute of **1**, which confers value upon its clinical use, is the very high affinity toward Fe(III), forming a stable 1:1 Fe(III):**1** hexadentate complex via the three hydroxamic acid functional groups ($\log\beta_{110}$ = 30.5).[16−18] The drawbacks of **1** have prompted research efforts to find orally available iron chelating agents.[5,6,19] Two of these candidates, deferiprone (1,2-dimethyl-3-hydroxypyrid-4-one, L1 (**2**)) and

*To whom correspondence should be addressed. Phone: +61-2-9351-6738. Fax: +61-2-9351-4717. E-mail: rcodd@med.usyd.edu.au.

[a]Abbreviations: AdAc, adamantane-1-acetic acid; AdA, adamantane-1-carboxylic acid; L_{DX}, 4-[3,5-bis(2-hydroxyphenyl)-1,2,4-triazol-1-yl]benzoic acid (deferasirox); DFOB, desferrioxamine B; AdA_{dMe}, 3,5-dimethyladamantane-1-carboxylic acid; ESI-MS, electrospray ionization mass spectrometry; ^{59}Fe-Tf, ^{59}Fe-labeled transferrin; AdA_{OH}, 3-hydroxyadamantane-1-carboxylic acid; Dp44mT, di-2-pyridyl ketone 4,4-dimethyl-3-thiosemicarbazone; MPOAc, 4-methylphenoxyacetic acid; L_{1D}, 3-hydroxy-2-methyl-4-oxo-1-pyridineacetic acid; NTBI, nontransferrin-bound-iron; ROS, reactive oxygen species; RP-HPLC, reversed-phase high pressure liquid chromatography.

 Published on Web 12/30/2009

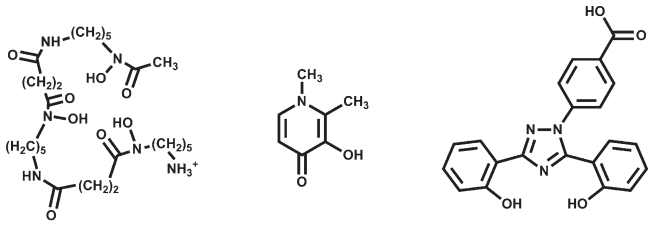

DFOB (**1**) deferiprone (**2**) deferasirox (**3**)

Figure 1. Schematic of the clinically used iron chelators used in this study: desferrioxamine B, DFOB (**1**); deferiprone (**2**); deferasirox (**3**).

deferasirox (4-[3,5-bis(2-hydroxyphenyl)-1,2,4-triazol-1-yl]-benzoic acid, ICL670 (**3**)) (Figure 1), both of which are orally active, have varied profiles in the clinic.[19−21]

Deferiprone (**2**) is an orally active, three-times-daily, α-ketohydroxypyridine-based bidentate iron chelator, which can remove iron from noncardiac parenchyma, macrophages, transferrin, ferritin, and hemosiderin.[19] Deferiprone is not as effective as **1** at removing Fe(III) and has toxicity issues, including agranulocytosis.[5,22,23] Its use is largely limited to the European Union as a second-line treatment for patients intolerant to **1**. Currently, **2** is not approved for use in the USA. Deferasirox (**3**) is a tridentate, one dose-per-day, orally administered iron chelator in use since 2005 in the USA, Switzerland, and Europe.[19,20] Deferasirox crosses hepatocyte and cardiac myocyte cell membranes and has shown good tolerance and safety with side effects that include mild gastrointestinal symptoms and mild aminotransferase elevation.[24,25] The first-in-class thiazolecarboxylic acid-based iron chelator, desferrithiocin, showed good iron clearance in monkeys but was severely nephrotoxic.[26,27] The less toxic derivative, deferitrin, showed favorable pharmacokinetics in rats, dogs, and monkeys[28] and is currently in phase II clinical trials.[19] Renal toxicity has also been observed in some patients treated with **3**.[29,30] The development of acceptable iron chelating drugs for iron overload, therefore, requires consideration of efficacy of Fe-binding, renal toxicity, and other potential side effects. Other drugs in development as iron chelators include the deferiprone derivative L1NA11,[19] hydroxypyridinone-based compounds,[31] isonicotinoyl hydrazones,[32−35] and thiosemicarbazones;[32,36−40] the latter two classes of compounds being developed principally as anticancer agents.

An alternative approach toward the design of new iron chelating compounds for the treatment of iron overload involves **1**-based semisynthesis, where ancillary compounds are appended to **1** via the free primary amine group, which itself is not involved in the Fe(III)-**1** coordination sphere.[17] In this approach, the integrity of the **1**-derived Fe(III)-binding hydroxamic acid groups of the conjugate are retained, yet the properties of the compound may be tuned as a function of the ancillary fragments. Conjugates of **1** have been previously prepared with a variety of groups appended at the amine terminus, including fluorophores,[41−44] ferrocene,[45] hydroxypyridinone-, or catecholate-based ligands[46−48] and others.[49−52] Most recently, the octanol−water partition coefficients of a series of alkylated **1** compounds were determined to be 200−3900 times that of free **1** at 25 °C.[51] This may have implications for improving the ability of free **1** to traverse cell membranes to access intracellular iron stores. Starch polymers of **1** have also been explored as a mechanism to improve the plasma half-life and toxicity.[52] In a more general context, conjugates of hydroxamic acid-based and catechol-based siderophores have a rich research profile as potential antibacterial and anticancer agents.[44,53,54]

Here, we describe the synthesis, characterization, and structure−activity relationships of seven DFOB conjugates (**4**−**10**, Figure 2). These studies include examination of the integrity of Fe(III)-binding using electrospray ionization mass spectrometry (ESI-MS) and reversed-phase high pressure liquid chromatography (RP-HPLC). We report the determination of the log*P* values of **4**−**10** in the absence and presence of Fe(III) and the iron chelation efficacy of **4**−**10** with regard to their ability to mobilize intracellular ^{59}Fe from SK-N-MC neuroepithelioma cells and to prevent ^{59}Fe uptake from ^{59}Fe-transferrin (^{59}Fe-Tf). Furthermore, we have examined the antiproliferative activity of **4**−**10** in SK-N-MC cells and in a renal epithelial cell type. Together, the results indicate that selected conjugates of **1** should be further evaluated as potential new agents for the treatment of iron overload disease.

Results and Discussion

Rationale for Chelator Design. Semisynthesis was used to prepare conjugates between **1** and lipophilic compounds with structures similar to those of selected orally available compounds in clinical use. Our rationale was that the favorable properties of the ancillary fragments (oral availability, lipophilicity, low toxicity) may be conferred upon the conjugates of **1**. We selected adamantane-1-carboxylic acid-based ancillary fragments for conjugation to **1**, with several compounds of this class in use clinically to treat influenza A (amantadine, rimantadine),[55] Parkinson's disease (amantadine),[56] Alzheimer's disease (memantine),[57] and pulmonary tuberculosis (*N*-adamantan-2-yl-*N*′-((2*E*)-3,7-dimethyl-2,6-octadien-1-yl)-1,2-ethanediamine (SQ109)).[58] Amantadine, rimantadine, and memantine are orally active and are generally well tolerated by patients. Among our target compounds, we included conjugates between **1** and (i) 4-methylphenoxyacetic acid, which mimics the internal fragment of the orally available compounds rosiglitazone and propranolol, (ii) 3-hydroxy-2-methyl-4-oxo-1-pyridineacetic acid, which mimics deferiprone (**2**), and (iii) deferasirox (**3**) itself.

Chemistry. 3-Hydroxy-2-methyl-4-oxo-1-pyridineacetic acid (L_{1D}), which is the *N*-acetic acid derivative of **2**, was prepared according to literature methods,[59,60] and the purity of the compound was confirmed by ^{1}H and ^{13}C NMR spectroscopy. Seven carboxylic acid derivatives, adamantane-1-carboxylic acid (AdA), 3-hydroxyadamantane-1-carboxylic acid (AdA_{OH}), 3,5-dimethyladamantane-1-carboxylic acid (AdA_{dMe}), adamantane-1-acetic acid (AdAc), 4-methylphenoxyacetic acid (MPOAc), L_{1D}, or 4-[3,5-bis(2-hydroxyphenyl)-1,2,4-triazol-1-yl]-benzoic acid (L_{DX}, **3**), were conjugated to **1** to yield **1**-AdA (**4**), **1**-AdA_{OH} (**5**), **1**-AdA_{dMe} (**6**), **1**-AdAc (**7**), **1**-MPOAc (**8**), **1**-L_{1D} (**9**), or **1**-L_{DX} (**10**), respectively (Figure 2). Initially, **4** was prepared via the conjugation of **1** with NHS-activated adamantane-1-carboxylic acid.[61] A more streamlined synthesis of **4**−**10** used HOBt-based, EDC-activated conjugation[62] (Scheme 1) and the compounds were purified to >95% using preparative RP-HPLC. Conjugation in each of **4**−**10** was evident from the absence in the ^{1}H NMR spectra of the amine group signal (δ = 2.7 ppm) of **1** and of the CO_2H signal in each of AdA, AdA_{OH}, AdA_{dMe}, AdAc, MPOAc, L_{1D}, or **3** ($\delta \sim$11.9 ppm). Additionally, the appearance of the signal due to the amide peak ($\delta \sim$ 7.3 ppm) and of the signals assigned to the ancillary ligands confirmed conjugation.

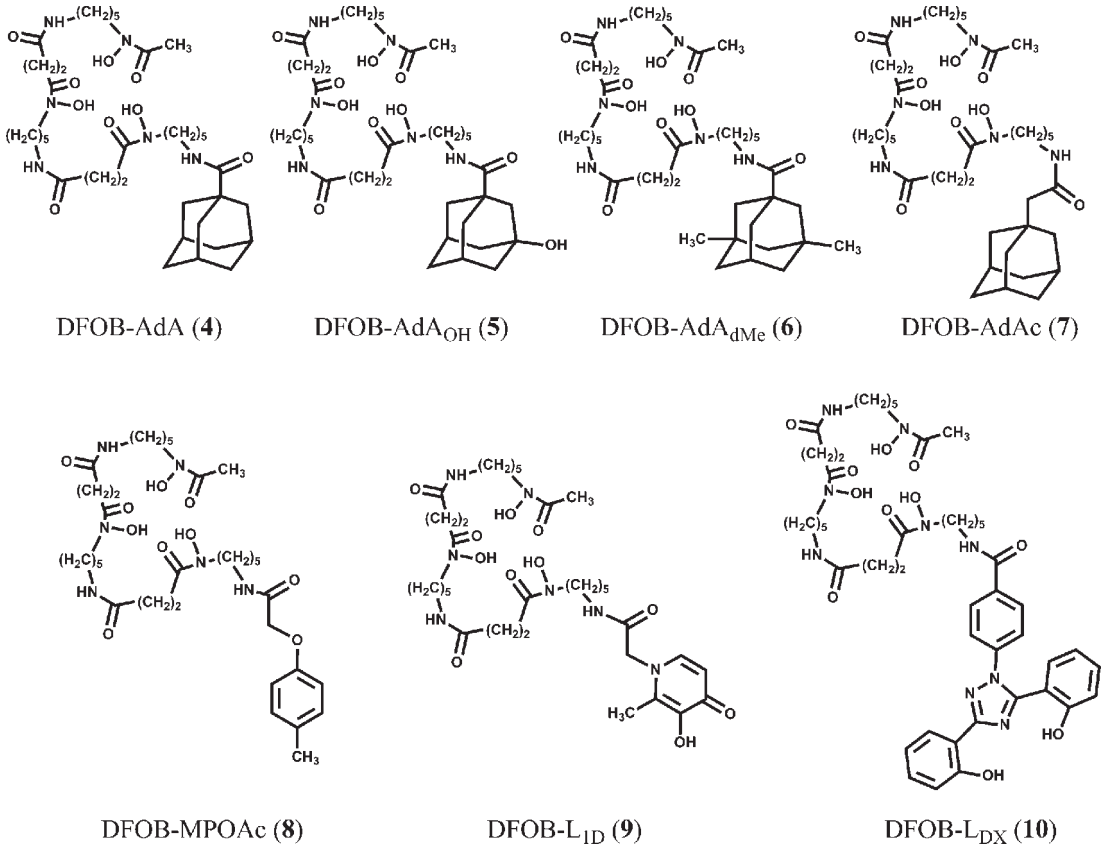

Figure 2. Schematic of the new DFOB conjugates prepared in this investigation: DFOB-AdA (**4**), DFOB-AdA$_{OH}$ (**5**), DFOB-AdA$_{dMe}$ (**6**), DFOB-AdAc (**7**), DFOB-MPOAc (**8**), DFOB-L$_{1D}$ (**9**), and DFOB-L$_{DX}$ (**10**).

Scheme 1. Synthesis of **4**−**10**

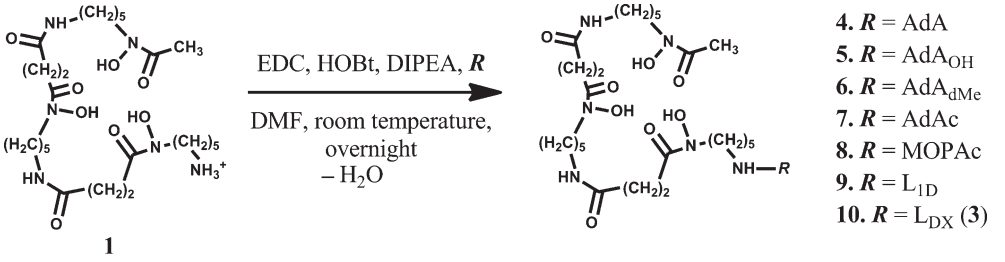

Charge of 4−10 in the Absence and Presence of Fe(III) and Fe(III)/(II) Redox Potentials. Upon the basis of the range of the pK_a values determined for the three hydroxamic acid-based protons of DFOB (pK_a 8.32−9.71)[63] and that compounds **4**−**8** have ancillary fragments with protons that will not ionize under biologically relevant conditions (as a reference point for **5**, 1-adamantanol pK_a = 18[64]), **4**−**8** will be neutral at physiological pH values. While compounds **9** and **10** have ancillary fragments with ionizable protons, the pK_a values of the hydroxyl group of **2** (pK_a = 9.75)[65,66] and of the phenolate groups of **3** (pK_a = 10.13 and 12.09)[67] prescribe that **9** and **10** will be neutral at physiological pH values. Therefore, **4**−**10** would be expected to be able to readily cross cell membranes as neutral species, which is likely to be favorable for accessing intracellular iron pools. The 1:1 complex formed between Fe(III) and the triple deprotonated DFOB fragment of **4**−**8** will also be neutral. Therefore, Fe(III)-loaded **4**−**8** are expected to exit the cell as neutral complexes. Depending upon metal:ligand stoichiometry, the charge of Fe(III)-loaded complexes of **9** and **10** may deviate from neutral. Upon the basis of the established coordination chemistry of Fe(III) and **2**[68] or **3**,[67,69] it is likely that there will be more than one type of Fe(III)-loaded complex formed with **9** and **10**.

The negative Fe(III)/(II) redox potentials reported for $[Fe(\mathbf{1}(3-))]^{+/0}$ ($E_{1/2}$ −0.48 V vs NHE at pH 7.5),[70,71] $[Fe(\mathbf{2}(1-))_3]^{0/1-}$ ($E_{1/2}$ −0.62 to −0.54 V vs NHE)[72] and $[Fe(\mathbf{3}(3-))_2]^{3-/4-}$ ($E_{1/2}$ −0.6 V vs NHE),[69] indicate that the Fe-loaded complexes of **4**−**10** will exist as redox stable Fe(III) complexes. Thus, it is unlikely that these complexes would engage in one-electron reduction reactions to yield the corresponding Fe(II) complexes under physiological conditions. Therefore, the possibility of the generation of ROS from Fe(II)-based Fenton reactions is unlikely for **4**−**10**. This enhances the potential for these compounds as Fe(III) chelators for iron overload rather than as iron chelators for cancer treatment.[32] The latter class of compounds, which includes di-2-pyridyl ketone 4,4-dimethyl-3-thiosemicarbazone (Dp44mT), are thought to depend upon Fe(III)/(II) redox cycling mechanisms for cytotoxicity.[32,33,36,37]

Table 1. ESI-MS Data (Positive Ion Mode) from **4**−**10** in the Absence and Presence of Fe(III)

		Fe(III) free			Fe(III) loaded		
compd	[M]	exp	calcd	species	exp	calcd	species
4	722.9	723.1	723.9	$[M + H^+]^+$	776.5	776.8	$[M - 3H^+ + Fe^{3+} + H^+]^+$
		745.3	745.9	$[M + Na^+]^+$	798.5	798.8	$[M - 3H^+ + Fe^{3+} + Na^+]^+$
		1467.5	1468.8	$[2\,M + Na^+]^+$			
5	738.9	737.2	739.9	$[M + H^+]^+$	792.5	792.8	$[M - 3H^+ + Fe^{3+} + H^+]^+$
					814.5	814.8	$[M - 3H^+ + Fe^{3+} + Na^+]^+$
6	751.0	751.1	752.0	$[M + H^+]^+$	804.5	804.8	$[M - 3H^+ + Fe^{3+} + H^+]^+$
					826.6	826.8	$[M - 3H^+ + Fe^{3+} + Na^+]^+$
7	736.9	737.4	737.9	$[M + H^+]^+$	790.6	790.8	$[M - 3H^+ + Fe^{3+} + H^+]^+$
		759.6	759.9	$[M + Na^+]^+$	812.6	812.8	$[M - 3H^+ + Fe^{3+} + Na^+]^+$
		782.3	781.9	$[M - H^+ + 2Na^+]^+$			
8	708.8	710	709.8	$[M + H^+]^+$	762.3	762.7	$[M - 3H^+ + Fe^{3+} + H^+]^+$
		732	731.8	$[M + Na^+]^+$	784.3	784.7	$[M - 3H^+ + Fe^{3+} + Na^+]^+$
		1439.2	1440.6	$[2\,M + Na^+]^+$	887.2	888.6	$[M - 3H^+ + Fe^{3+} + H^+]^+ \cdot 2NaCl \cdot 0.5H_2O$
9	725.8	727	726.8	$[M + H^+]^+$	868.1	868.9	$[M - 4H^+ + 2Fe^{3+} + Cl^-]^+$
		748.5	748.8	$[M + Na^+]^+$			
10	916.0	916.5	917.0	$[M + H^+]^+$	1022.2	1022.7	$[M - 5H^+ + 2Fe^{3+}]^+$
		938.7	939.0	$[M + Na^+]^+$			

Fe(III) Coordination. The Fe(III) coordination of **4**−**10** was examined using ESI-MS (Table 1), electronic absorption spectroscopy, and RP-HPLC measurements. For Fe(III)-loaded solutions of **4**−**7**, the dominant species in the positive ion ESI-MS formulated as the protonated ($[M - 3H^+ + Fe^{3+} + H^+]^+$) or sodiated ($[M - 3H^+ + Fe^{3+} + Na^+]^+$) form of the intrinsically uncharged species, $[M - 3H^+ + Fe^{3+}]$, in which Fe(III) was bound to the triple deprotonated **1** motif. For **8**, the $[M - 3H^+ + Fe^{3+} + H^+]^+$ and $[M - 3H^+ + Fe^{3+} + Na^+]^+$ ions were present in low abundance (both ∼12%), with the major signal (100%) ascribed to $[M - 3H^+ + Fe^{3+} + H^+]^+ \cdot 2NaCl \cdot 0.5H_2O$. The Fe(III):ligand ratio of 1:1 for **4**−**8** determined from ESI-MS measurements was also established from Job's plots analyses. The isotope pattern of the signal at m/z = 868.1 for Fe(III)-loaded **9** simulated as $[M - 4H^+ + 2Fe^{3+} + Cl^-]^+$ ($[C_{33}H_{51}N_7O_{11}ClFe_2]^+$ requires 868.9). For Fe(III)-loaded **10**, the observed isotope pattern (m/z = 1022.2) was consistent with $[M - 5H^+ + 2Fe^{3+}]^+$ ($[C_{46}H_{56}N_9O_{11}Fe_2]^+$ requires 1022.7) (Figure 3). For **9** and **10**, which feature pendant groups with the capacity to bind iron, it is possible that species exist where the metal:ligand ratio is >1. This is evident from the ESI-MS analysis, with Fe(III):**9** or **10** = 2:1, indicating that **9** and **10** could potentially carry a greater than stoichiometric load of Fe.

Under iron saturation, Fe(III)-loaded **9** or **10** could yield $[Fe_4(\mathbf{9}(4-))_3]$ or $[Fe_3(\mathbf{10}(5-))_2]^-$, respectively (Figure 4). The argument against Fe(III)-saturated complexes of **9** and **10** as efficacious Fe mobilizing agents relates to the high molecular weights of each of these complexes, $[Fe_4(\mathbf{9}(4-))_3]$ (M_r = 2388.8 g mol^{-1}) and $[Fe_3(\mathbf{10}(5-))_2]^-$ (M_r = 1989.6 g mol^{-1}), which may impede cellular efflux. Models of Fe(III)-loaded complexes of **1**−**10** were built in HyperChem 7.5 using data from X-ray crystal structures of $[Fe(\mathbf{1}(3-))]^+$,[17] 2,5-dioxopyrrolidin-1-yl adamantane-1-carboxylate,[61] $[Cr(\mathbf{2}(1-))_3]$,[73] and [Fe{(3,5-bis(2-hydroxyphenyl)-1-phenyl-1,2,4-triazole)-(2−)}$_2$].[69] The volumes of $[Fe_4(\mathbf{9}(4-))_3]$ (5335 Å^3) and $[Fe_3(\mathbf{10}(5-))_2]^-$ (4436 Å^3) were significantly greater than the volume of $[Fe(\mathbf{6}(3-))]$ (1984 Å^3). The size and shape of the Fe(III) complex may be an important structure−activity relationship with regard to the ability of **9** and **10** to mobilize cellular Fe, although the variable stoichiometry of Fe(III):**9** or **10** complexes makes it difficult to establish such a relationship with certainty.

RP-HPLC of Compounds in the Absence and Presence of Fe(III). All compounds were purified by preparative scale RP-HPLC because the modest solubility of **4**−**10** in water or methanol prevented purification by recrystallization or flash chromatography. A single major peak was observed in the analytical RP-HPLC of **4**−**10**, which demonstrated that the purity of the compounds was >95% (Figure 5). In the presence of Fe(III), the values of the retention time (t_r) of the peaks attributable to Fe(III)-loaded **4**−**9** decrease (range of 0.5 min (**6**) to 2.1 min (**9**)), which indicates that the Fe(III)-loaded complexes are more water-soluble that the free ligand. This is consistent with the function of bacterial siderophores in nature to increase the aqueous solubility of Fe(III) under aerobic conditions[10] and with the decrease in log$D_{7.4}$ values for Fe(III)-loaded complexes of **1**−**3**, relative to the values of the respective free ligands.[74]

Two peaks eluted in the RP-HPLC trace of a solution of Fe(III)-loaded **9** (t_r 12.2 and 10.9 min). Analysis from RP-HPLC-MS (positive ion mode) showed a distribution of Fe(III)-loaded **9** species. The HPLC-MS trace from the fraction eluting at t_r = 12.2 min yielded signals at m/z: 390.32 (60), m/z 416.79 (1), 779.22 (100), and 1557.90 (5), corresponding to $[M - 3H^+ + Fe^{3+} + 2H^+]^{2+}$ (m/z_{calc} 390.34), $[M - 3H^+ + 2Fe^{3+} - H^+]^{2+}$ (m/z_{calc} 416.75), $[M - 3H^+ + Fe^{3+} + H^+]^+$ (m/z_{calc} 779.67), and $[M - 4H^+ + Fe^{3+} + M - H^+ + Fe^{3+}]^+$ or $[2(M - 3H^+ + Fe^{3+}) + H^+]^+$ (m/z_{calc} 1558.34), respectively. The major Fe(III)-**9** species present in the fraction eluting at t_r = 12.2 min occurred as 1:1 or 2:2 species. The HPLC-MS trace from the fraction eluting at t_r = 10.9 min yielded signals at m/z 390.32 (60), m/z 416.79 (100), 779.22 (75), 868.09 (25), and 946.04 (40). The latter two signals were unique to the peak eluting at t_r = 10.9 min and corresponded with $[M - 3H^+ + 2Fe^{3+} - H^+ + Cl^-]^+$ (m/z_{calc} 868.96) and $[M - 3H^+ + 2Fe^{3+} + SO_4^{2-} 0.5CH_3OH]^+$ (m/z_{calc} 946.61). The three major Fe(III)-**9** species present in the peak eluting at t_r = 10.9 min occurred as 2:1 species. Therefore, the HPLC-MS analysis indicated that there was a distribution of Fe(III)-**9** species present with different Fe(III):ligand ratios with charges that may contribute a distribution coefficient (log$D$) based effect upon the t_r values in the RP-HPLC for the two groups of species. In support of this idea is the Job's plot analysis for **9**, which showed diffuse isosbestic points at 260, 310, and 370 nm,

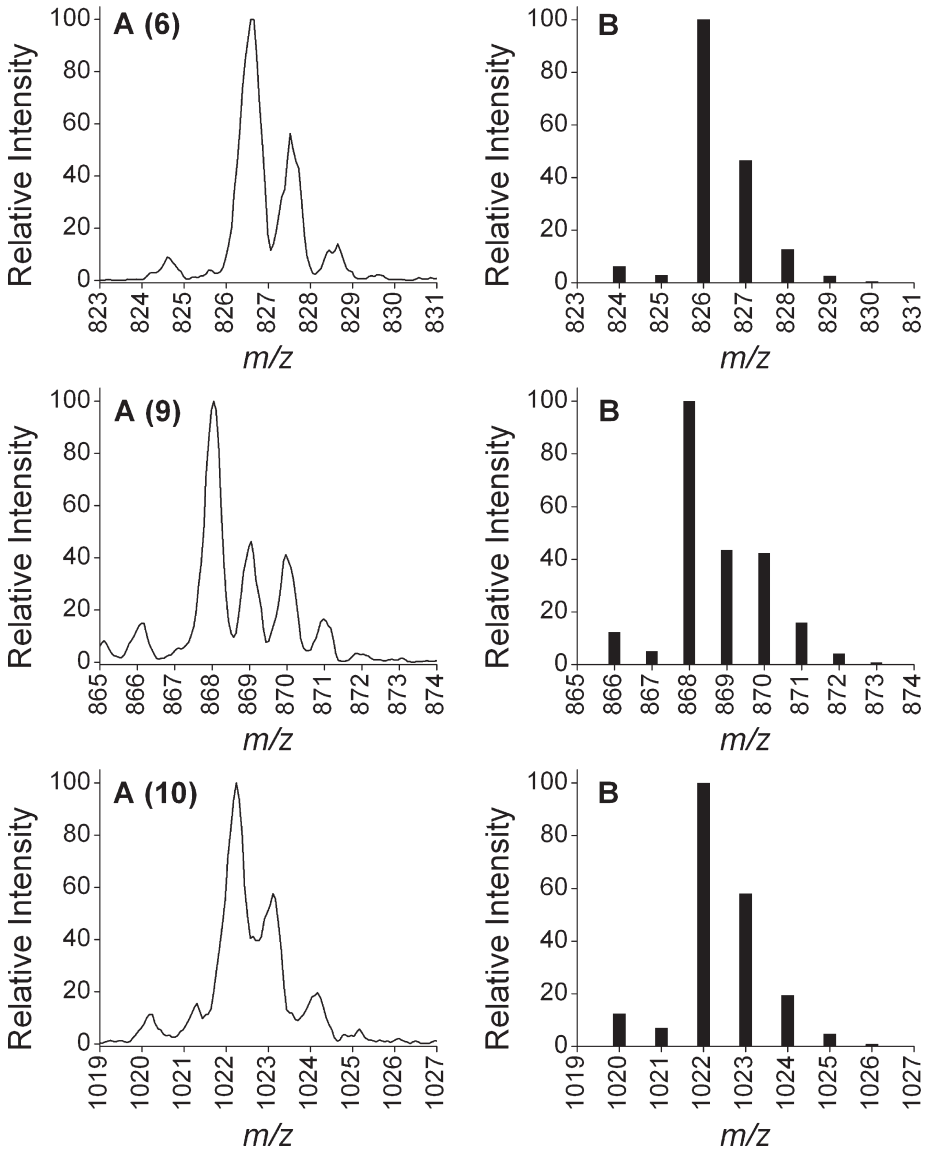

Figure 3. ESI-MS (positive ion) from Fe(III)-loaded solutions of **6**, **9**, or **10** as experiment (A) and (B) simulated. For **6**, *m*/*z* 826.6 (obs) $[M - 3H^+ + Fe^{3+} + Na^+]^+$ requires 826.8 (calcd) $[C_{38}H_{63}N_6O_9FeNa]^+$. For **9**, *m*/*z* 868.1 (obs) $[M - 4H^+ + 2Fe^{3+} + Cl^-]^+$ requires 868.9 (calcd) $[C_{33}H_{51}N_7O_{11}ClFe_2]^+$. For **10**, *m*/*z* 1022.2 (obsd) $[M - 5H^+ + 2Fe^{3+}]^+$ requires 1022.7 (calcd) $[C_{46}H_{56}N_9O_{11}Fe_2]^+$.

indicative of the presence of more than two species in solution. A distribution of species formed between Fe(III) and **2** has been detected within the limits of ESI-MS,[68] which further supports the presence of more than one species in solutions of Fe(III) and **9**.

For **10**, there was not a clear shift in the retention time of the peak ascribed to Fe(III)-loaded **10** compared to the free ligand. However, Fe(III) binding was evident from the significant change in the absorbance value of the peak of Fe(III)-loaded **10**. The absorbance value at 220 nm of an electronic absorption spectrum from a 1:1 Fe(III):**10** solution (0.1 mM) and **10** (0.1 mM) from the Job's plot analysis was 1.8 and 0.15, respectively. A similar fold difference in absorbance was observed in the RP-HPLC traces of **10** in the absence and presence of Fe(III). The phenomenon of a change in electronic absorption spectrum but not in RP-HPLC retention time for hydrophobic siderophores has been reported for those derived from bacteria.[75] The apex of the major peak from a solution of Fe(III)-loaded **10** analyzed by RP-HPLC-MS (positive-ion mode) gave a signal at $m/z = 969.29$, which corresponded to $[M - 3H^+ + Fe^{3+} + H^+]^+$. The sloping front of the peak gave a signal at $m/z = 1022.13$, which corresponded to $[M - 5H^+ + 2Fe^{3+}]^+$, as observed in the ESI-MS experiments (Table 1). Therefore, similarly to Fe(III)-loaded **9**, there appeared to be a distribution of species of Fe(III)-loaded **10**, which accords with the complex pH-dependent species distribution previously observed for **3**.[69]

Determination of Log*P* Values of 4−10. The t_r values for **4**−**10** were greater than the t_r value of **1**, which is congruous with the predicted increase in the log*P* values of **4**−**10**, compared to **1**. The water solubility of **1** is attributable, in part, to the charged amine group at physiological pH values. The charge neutrality of **4**−**10**, in addition to the lipophilicity inherent to the ancillary fragments (Figure 2), would expect to yield compounds that are more lipophilic than the parent **1**. Previous work has shown this to be the case for alkylated adducts of **1**.[51]

The log*P* values of **4**−**10** in the absence and presence of Fe(III) were estimated using RP-HPLC (Table 2). This

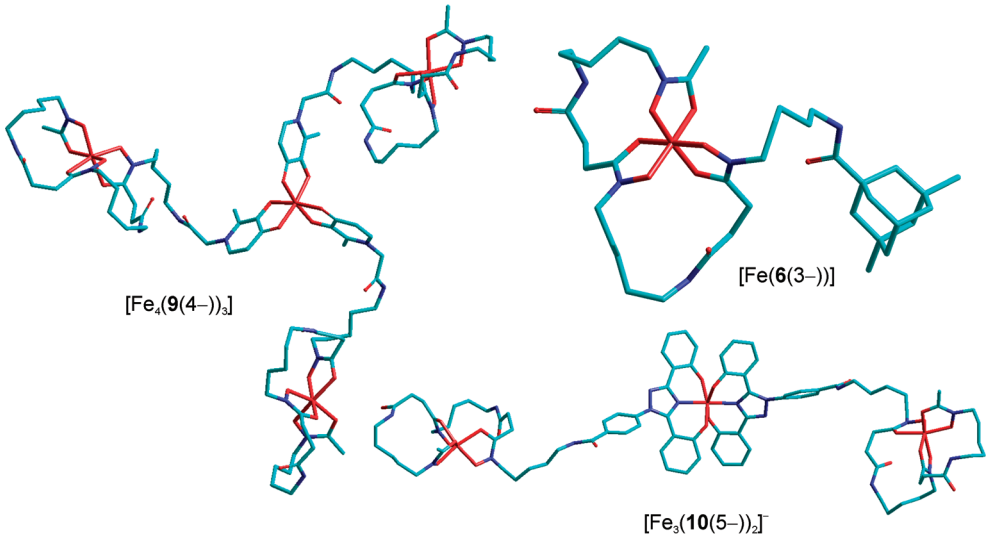

Figure 4. Models built using HyperChem 7.5 of [Fe(**6**(3−))], [Fe_4(**9**(4−))$_3$] and [Fe_3(**10**(5−))$_2$]$^-$ based on data from X-ray crystal structures of related fragments.[17,61,69,73] Hydrogen atoms have been omitted for clarity.

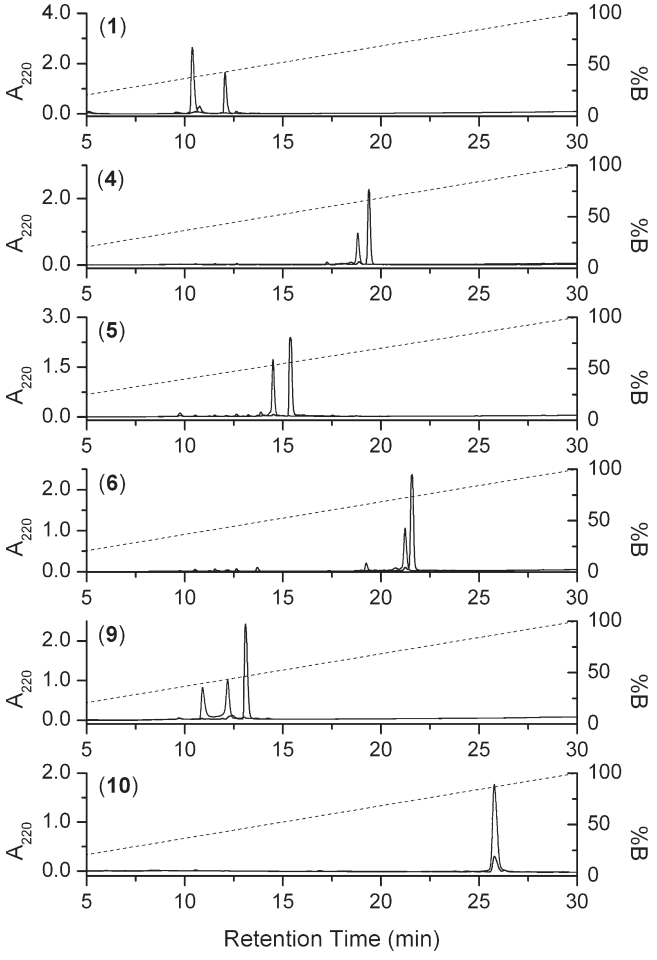

Figure 5. RP-HPLC traces of **1**, **4**, **5**, **6**, **9**, and **10** in the absence (black) or presence (gray) of Fe(III).

method is valid in this case because, under the conditions used for RP-HPLC measurements, **4**−**10** will be neutral and there will be no log*D* contribution to the log*P* values. For neutral, Fe(III)-loaded complexes of **4**−**8**, the log*P* values will also be valid, as determinable via RP-HPLC. However, due to the non-neutral charge on Fe(III)-loaded **9** and **10**, log*P* values are not able to be calculated reliably using RP-HPLC, alongside values for **1**−**3** and for Fe(III)-loaded **1**−**3**. The t_r values for **4**, **6**−**8**, and **10** fell within or close to the t_r values of the four standard compounds used to generate the regression analysis.[76] For **5** and **9**, the t_r values fell outside the range of the standards, which prompted parallel determinations of log*P* values for **4**−**10** using the shake-flask method. The experimentally determined log*P* values for **4**−**10** using both RP-HPLC and shake-flask methods compared reasonably well (Table 2) and were also in broad agreement with log*P* values calculated using Advanced Chemistry Development Software V8.14 or for models of **4**−**10** that were built using HyperChem 7.5 (Table 2).

Cellular ^{59}Fe Mobilization. The ability of **1**−**10** and Dp44mT to mobilize intracellular ^{59}Fe from human SK-N-MC neuroepithelioma cells prelabeled with ^{59}Fe-Tf was examined (Figure 6A). The Fe metabolism of this cell type and the effect of a variety of chelators on this cell type is well characterized,[77,78] which underscores its choice for measuring Fe mobilization. The ability of **1** ($\log P_{(av)} = -2.1$) to induce the mobilization of intracellular ^{59}Fe is rather modest (12 ± 1%), relative to control medium alone (5 ± 1%; Figure 6A). This is consistent with our previous findings using this assay where DFOB·mesylate was unable to readily access intracellular iron stores over short incubation times.[77,78]

Of the four adamantane-1-carboxylic acid-based conjugates of **1**, three compounds (**4**, **6**, and **7**) were effective in increasing the mobilization of intracellular ^{59}Fe in comparison to free **1** by factors of 2.2, 3, and 2.8, respectively. Compound **6** increased ^{59}Fe release to an extent that was comparable ($p > 0.05$) to the positive controls, **3**, and Dp44mT (Figure 6A). Compound **7** showed ^{59}Fe mobilizing efficacy comparable ($p > 0.05$) to that of **3**. In contrast, **5** showed activity that was similar to control medium and was significantly ($p < 0.001$) less efficient as an ^{59}Fe mobilizing agent than **1**.

Because no major steric or electronic perturbations were made to the **1** motif of the monofunctional **1**-adamantyl adducts **4**−**7**, the affinities of **4**−**7** toward Fe(III) will be similar to the affinity between **1** and Fe(III) ($\log\beta_{110} = 30.5$).[16,17] These values, or the pFe(III) values (pFe(III) =

Table 2. Log*P* Values of **1**−**10** in the Absence and Presence of Fe(III) as Determined from RP-HPLC, the Shake-Flask Method, and from Calculation

	Fe(III) free						Fe(III) loaded		
compd	t_r (min)[b]	LogP_{exp}[c]	LogP_{exp}[d]	LogP_{calc}[e]	LogP_{calc}[f]	LogP_{av}	t_r (min)[b]	LogP_{exp}[c]	V (Å^3)
1	12.04	NC[g]	ND	−2.74	−1.45	−2.10 ± 0.91	10.40	NC	1470
2	ND[h]	ND	−1.02[i]	−0.22	−0.81	−0.68 ± 0.41	ND	ND	1155
3	25.43	NC	3.8[j]	6.43	5.18	5.14 ± 1.32	25.39	NC	1766
4	19.31	1.29	2.11	ND	1.35	1.58 ± 0.46	18.56	1.04	1903
5	15.39	−0.11	0.29	ND	0.11	0.10 ± 0.20	14.51	−0.48	1922
6	21.54	1.95	2.92	ND	2.22	2.36 ± 0.50	21.08	1.82	1984
7	19.92	1.47	2.21	ND	1.28	1.65 ± 0.49	19.38	1.31	2002
8	18.21	0.93	1.68	ND	0.80	1.14 ± 0.48	17.48	0.68	1918
9	13.04	−1.16	−1.29	ND	−0.66	−1.04 ± 0.33	10.93	NC	5335[k]
							12.23	NC	
10	25.8	3.02	2.17	ND	4.17	3.12 ± 1.00	25.8	NC	4436[l]
BDME[a]	20.02	ND	1.61[m]	1.64	1.51	1.59 ± 0.07	ND	ND	ND
BDEE[a]	24.09	ND	2.54[m]	2.70	2.19	2.48 ± 0.26	ND	ND	ND
NAPH[a]	26.99	ND	3.32	3.45	3.05	3.27 ± 0.20	ND	ND	ND
DBFN[a]	28.88	ND	4.04	4.12	3.11	3.76 ± 0.56	ND	ND	ND

[a] BDME = 1,2-benzenedicarboxylic acid 1,2-dimethyl ester; BDEE = 1,2-benzenedicarboxylic acid 1,2-diethyl ester; NAPH = naphthalene; DBFN = dibenzofuran. [b] t_o = 1.81 min. [c] Determined from RP-HPLC (multiple runs showed reproducibility; given data is from a single series of experiments). [d] Determined from shake-flask. [e] As reported as calculated using Advanced Chemistry Development Software V8.14.on SciFinder Scholar Database. [f] Calculated from models built using HyperChem 7.5. [g] NC = not calculable. [h] ND = not determined. [i] From ref 91. [j] From ref 92. [k] Modeled for Fe(III) saturated 9:Fe(III) = 3:4 complex (Figure 4). [l] Modeled for Fe(III) saturated 10:Fe(III) = 2:3 complex (Figure 4). [m] From ref 93.

−log[Fe(III)] when $[Fe(III)]_{total} = 10^{-6}$ M and $[ligand]_{total} = 10^{-5}$ M at pH 7.4; for **1**, pFe(III) = 26),[79] are not expected to differ significantly among this subgroup of compounds. Therefore, the decreased release of ^{59}Fe mediated by **5**, compared to the ^{59}Fe mobilization mediated by **4**, **6**, and **7**, suggests the efficacy of a chelator is not solely determined by the affinity toward Fe(III). In fact, multiple factors are involved in terms of optimal Fe chelation efficacy, as found for other types of ligands.[80]

Of the remaining **1** conjugates (**8**, **9**, and **10**), **8** and **10** showed significantly ($p < 0.001$) greater ^{59}Fe cellular efflux activity than **1**. The conjugate between L_{1D} and **1** (**9**) demonstrated little activity, not being significantly ($p > 0.05$) more active that control medium at mobilizing ^{59}Fe from cells. Compared to the control, the clinically used orally active chelator, L1 (**2**), also showed little ability to mobilize ^{59}Fe (Figure 6A) and was less effective than the other positive controls (**1**, **3** and Dp44mT). Previous studies using a similar protocol have demonstrated that relatively high concentrations of L1 (i.e., 0.5 mM) are necessary to induce only moderate ^{59}Fe mobilization from cells.[81] Hence, in terms of structure−activity relationships, conjugates between **1** and **2** do not appear optimal. The conjugate between **1** and **3** (**10**) showed ^{59}Fe mobilization efficacy that was significantly ($p < 0.001$) less effective than **3** alone.

An ideal iron chelating molecule for iron overload treatment should have properties that allow the compound to: (i) cross the cell membrane to access intracellular iron stores, (ii) selectively form a redox-inactive Fe(III) complex, and (iii) exit the cell as a stable, Fe(III)-loaded complex for excretion.[7,32] Criteria (i) and (iii) are described in part by the charge and the partition coefficient of the free compound and of the Fe(III)-loaded complex, respectively, and criterion (ii) is described by the thermodynamics and kinetics of Fe(III) coordination. In the case of some of the **1** conjugates (namely, **4**, **6**−**8**), these properties have been favorably altered in comparison to **1**. In contrast, for other conjugates such as **5** and **9**, structure−activity relationships involving properties such as relatively low log*P* values and/or the high molecular weight of Fe(III)-loaded complexes may explain the hindered membrane permeability and, thus, Fe chelation efficacy.

Inhibition of Cellular ^{59}Fe Uptake from ^{59}Fe-Transferrin. The ability of **1**−**10** or Dp44mT to prevent the internalization of ^{59}Fe from ^{59}Fe-Tf was analyzed in the human SK-N-MC neuroepithelioma cell line (Figure 6B). Generally, these results reflected those of the intracellular ^{59}Fe mobilization study (Figure 6A), demonstrating that compounds with high ^{59}Fe mobilization efficacy were also efficient at preventing the uptake of ^{59}Fe from ^{59}Fe-Tf. The ability of **1** to prevent ^{59}Fe uptake from ^{59}Fe-Tf was poor, inhibiting ^{59}Fe uptake to 87% of the control (Figure 6B), as shown in previous studies.[77,78] Of the compounds in this work, **4**, **6**−**8**, and **10** were significantly ($p < 0.01$) more active than **1**. Compound **6** was the most efficient compound, inhibiting ^{59}Fe uptake from ^{59}Fe-Tf to 18 ± 2% of the untreated control. This efficiency was significantly ($p < 0.001$) greater than the positive control **3**, which reduced ^{59}Fe uptake to 39 ± 2% of the control and was slightly less effective than the highly potent antitumor chelator, Dp44mT, which inhibited ^{59}Fe uptake to 12 ± 1% of the control.

In summary, examining both the Fe efflux and Fe uptake studies (Figure 6A,B), the most effective **1** conjugates in terms of Fe chelation efficacy were **4**, **6**, **7**, and **10**, with activities that are at least twice that of **1**.

Structure−Activity Relationship between Log*P* Values and ^{59}Fe Mobilization. A parabolic relationship is evident between the log*P* values of **4**−**10** and the cellular efflux of ^{59}Fe (Figure 7A), giving an optimal log*P* value of 2.3 for maximal Fe efflux. The data from **1**, **2**, and Dp44mT[36] also fit well onto this parabola, with data for **3** an outlier. Because the descending parabola is described by only one data point with a broad error margin (**10**), there is some uncertainty as to whether the relationship between the log*P* values and ^{59}Fe efflux is truly parabolic. However, the ascending data is populated by sufficient data points to claim at least a sigmoidal relationship between ^{59}Fe efflux and log*P* values <2.3. This optimal log*P* value for Fe mobilization is also supported by the parabolic, or at a minimum, sigmoidal relationship, between log*P* and ^{59}Fe uptake from ^{59}Fe-Tf (Figure 7B). Thus, the lipophilicity of the chelator appears to be an important factor in determining the ability of the ligand to mobilize cellular Fe.

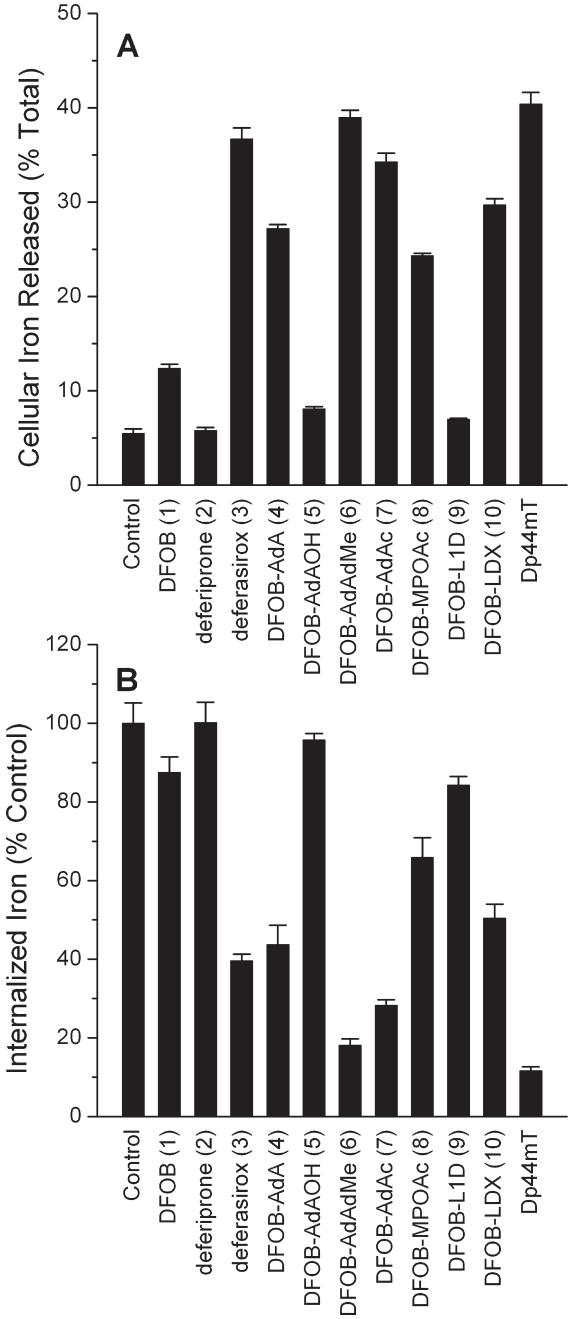

Figure 6. The effect of the new DFOB conjugates (**4**−**10**) in comparison with the clinically used chelators DFOB (**1**), deferiprone (**2**), deferasirox (**3**), or Dp44mT on: (A) cellular ^{59}Fe released (%) from human SK-N-MC neuroepithelioma cells prelabeled with ^{59}Fe-transferrin (^{59}Fe-Tf), or (B) ^{59}Fe uptake (% of control) from ^{59}Fe-transferrin (^{59}Fe-Tf) by SK-N-MC neuroepithelioma cells. Results are mean ± SD of three experiments with three determinations in each experiment.

Cell Viability. The ability of selected compounds from **1**−**10** and Dp44mT to inhibit cellular proliferation of Madin−Darby canine kidney type II (MDCK II) cells and human SK-N-MC neuroepithelioma cells was assessed using the [3-(4,5-dimethylthiazol-2-yl)-2,5-diphenyltetrazolium bromide] (MTT) assay[82] (Table 3). Compounds that are well tolerated by cells will not affect regular cellular proliferation or growth and will have high IC_{50} (or LD_{50}) values relative to more cytotoxic compounds. The cell viability data using the human SK-N-MC neuroepithelioma cell type reflects similar

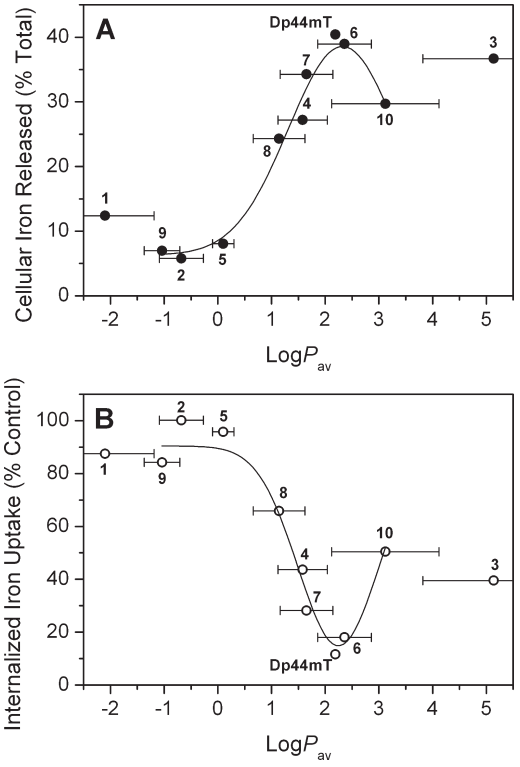

Figure 7. Log*P* values (average of values determined by RP-HPLC, shake-flask, and calculation) of **1**−**10** and Dp44mT as a function of (A) cellular ^{59}Fe released (%) from human SK-N-MC neuroepithelioma cells prelabeled with ^{59}Fe-transferrin (^{59}Fe-Tf) or (B) ^{59}Fe uptake (% of control) from ^{59}Fe-transferrin (^{59}Fe-Tf) by SK-N-MC neuroepithelioma cells.

Table 3. IC_{50} Values (μM) of **1**−**10** and Dp44mT in Madin−Darby Canine Kidney Type II (MDCK II) or in SK-N-MC Neuroepithelioma cell types

		IC_{50} (μM)	
	compd	MDCK II canine kidney	SK-N-MC neuroepithelioma
1	DFOB	9.49 ± 1.24	16.04 ± 0.47
2	deferiprone	ND[a]	165.88 ± 1.90
3	deferasirox	ND[a]	20.54 ± 0.56
4	DFOB-AdA	118.86 ± 1.16	174.04 ± 1.61
5	DFOB-AdA_{OH}	>100	>200
6	DFOB-AdA_{dMe}	163.37 ± 1.52	92.36 ± 1.66
7	DFOB-AdAc	225.56 ± 1.28	167.14 ± 2.82
8	DFOB-MPOAc	>150	>200
9	DFOB-L_{1D}	>300	>200
10	DFOB-L_{DX}	23.41 ± 1.53	20.62 ± 1.79
	Dp44mT	ND[a]	0.01 ± 0.01

[a] ND = not determined.

trends as observed in the MDCK II cell line. Importantly, in both cell types, all of the **1** conjugates (**4**−**10**) showed less cytotoxicity than **1**. Moreover, the most active **1** conjugates at mobilizing ^{59}Fe from cells and reducing cellular ^{59}Fe uptake from ^{59}Fe-Tf, namely **4**, **6**, **7**, and **10**, were significantly ($p < 0.005$) less cytotoxic than **1**, demonstrating that these compounds are highly tolerated and do not remove cellular Fe pools vital for cellular proliferation. This low antiproliferative activity is vital in the design of an iron chelator for the treatment of iron overload. The antiproliferative activity of all of the **1** conjugates are 1600 to >20000 times less effective than the known cytotoxic iron chelator, Dp44mT (IC_{50} 0.01 μM; Table 3).[40] Hence, this analysis

suggests that the **1** conjugates are more appropriate for the treatment of iron overload disease rather than cancer. Finally, a recent study showed a positive correlation between the log*P* value and toxicity of desferrithiocin analogues.[27] For **4**−**10**, no structure−activity relationships were evident between log*P* and toxicity.

Conclusions

The high solubility of **1** in water, which impacts negatively on its biological activity, can be significantly reduced by conjugating an ancillary fragment to the amine group of **1** without adversely affecting the Fe(III) coordinating ability of the conjugate. This is a crucial structure−activity relationship that may be useful to exploit in the future. We conjugated to **1**: (i) polycyclic-cage based compounds (adamantane-based derivatives), which have analogues in the clinic (amantadine, rimantadine, and memantine) that are orally active and that are generally well-tolerated by patients, (ii) 4-methylphenoxyacetic acid, and (iii) a deferiprone mimic (3-hydroxy-2-methyl-4-oxo-1-pyridineacetic acid), and deferasirox itself. Given that the affinity toward Fe(III) will not vary significantly among **4**−**8**, the relatively poor Fe mobilization ability of **5** illustrates that Fe(III) affinity is not the sole determinant of Fe chelating efficacy. From Fe efflux and Fe uptake studies, **4**, **6**, **7**, and **10** were at least twice as active as **1** with regard to Fe chelation efficacy and were significantly less cytotoxic than **1**, as determined using two different cell types. Therefore, these compounds may have promise as compounds for the treatment of iron overload disease rather than as anticancer agents. Neurological conditions that have been associated with transition metal ion dys-homeostasis, such as Parkinson's disease, Alzheimer's disease, and Huntington's disease,[83] or other conditions that have shown benefits from treatment via Fe chelation, such as malaria,[41,84] could also be potentially targeted by this class of compounds.

Experimental Section

Chemical Studies. Chemicals. Desferrioxamine B·mesylate (DFOB, 95%), 3-hydroxy-2-methyl-4-pyrone (maltol, 99%), glycine (>99%) adamantane-1-carboxylic acid (AdA, >99%), 3-hydroxyadamantane-1-carboxylic acid (AdA_{OH}, 97%), 3,5-dimethyladamantane-1-carboxylic acid (AdA_{dMe}, 97%), adamantane-1-acetic acid (AdAc, 98%), 4-methylphenoxyacetic acid (MPOAc, 98%), *N*-(3-dimethylaminopropyl)-*N*′-ethylcarbodiimide·HCl (EDC, protein sequence grade), $Fe(ClO_4)_3 \cdot H_2O$, dimethylformamide (DMF, biotech grade), and acetonitrile (CH_3CN, biotech grade) were obtained from Sigma-Aldrich (St. Louis, MO). 1-Octanol (99.5% GC grade) was from Fluka (Buchs, Switzerland). *N*-Hydroxybenzotriazole (HOBt) was obtained from Auspep (Parkville, VIC, Australia), and 4-[3,5-bis-(2-hydroxyphenyl)-1,2,4-triazol-1-yl]benzoic acid (L_{DX}, deferasirox) was obtained from AmplaChem (Carmel, IN). *N*,*N*-Diisopropylethylamine (DIPEA) (99%) was purchased from Lancaster Synthesis, Inc. (Pelham, NH), and methanol (99%) was obtained from Mallinckrodt Chemicals (Phillipsburg, NJ). All chemicals and solvents were used as received.

General Instrumentation. ^{1}H Nuclear magnetic resonance spectra were recorded using a Bruker Avance DPX 200 (Rheinstetten, Germany) at a frequency of 200.13 MHz or a Bruker Avance DPX 300 at a frequency of 300.10 MHz. Chemical shifts are reported as parts per million (ppm) with DMSO-d_6 (δ_H = 2.50) or CD_3OD (δ_H 3.31) used as an internal reference. ^{13}C Nuclear magnetic resonance spectra were recorded using a Bruker Avance DPX 200 spectrometer at a frequency of 50.3 MHz or a Bruker Avance DPX 300 at a frequency of 75.5 MHz. Electron spray ionization mass spectra (ESI-MS) were recorded using positive ionization on a Finnigan LCQ or a Finnigan MAT 900 XL ion trap mass spectrometer (San Jose, CA) with the following parameters. Mobile phase, methanol; flow rate, 0.30 mL min^{-1}; injection volume, 25 μL, spray voltage, 4.50 kV; capillary voltage, 35 V; capillary temperature, 210 °C; tube lens-offset, 10 V. Analytical thin layer chromatography (TLC) was performed using precoated silica gel plates (Sigma-Aldrich), which were eluted with MeOH:$CHCl_3$ = 1:3 and visualized using solid iodine or by dipping the plate into an ethanolic solution of $FeCl_3$ (60 mM). Reversed-phase high pressure liquid chromatography (RP-HPLC) used a Waters system (Milford, MA) consisting of a GBC 1460 degasser, a Rheodyne 7725i injector (analytical 20 μL loop, preparative 1700 μL loop) (Apple Valley, MN), a Waters 486 tunable absorbance detector, and a Waters Empower 2 software with Waters Sunfire C18 columns (particle size 5 μm, column dimension 4.6 mm × 150 mm i.d. (analytical), or particle size 5 μm, column dimension 19 mm × 150 mm i.d. (preparative)) and a flow rate of 0.2 mL/min (analytical) or 7.0 mL/min (preparative), with a mobile phase of water (0.1% TFA, solvent A) and acetonitrile (0.1% TFA, solvent B). HPLC-MS was conducted on a Thermo Separation system with a ThermoQuest Finnigan LCQ Deca mass spectrometer (San Jose, CA, USA).

General Procedure. 3-Hydroxy-2-methyl-4-oxo-1-pyridineacetic acid (L_{1D}) was synthesized according to the literature[59,60] from an aqueous solution (75 mL) of glycine (30 g, 400 mmol), maltol (12.7 g, 100 mmol), and NaOH (11 g, 275 mmol), which was reacted at 35 °C for 5 d. The solution was acidifed with 5 M HCl (4 mL) and was refrigerated for 2 h to yield a cream colored residue, which was filtered and washed with cold water. The solid product was redissolved in basic aqueous solution (pH 10.8) using 2 M NaOH (20 mL) and was acidified with 5 M HCl (4 mL) to give L_{1D} as a pale-white solid (3.28 g, 18%). ^{1}H NMR (300 MHz, DMSO-d_6) δ_H: 7.3 (1H, s, OH), 2.1 (3H, s, CH), 1.9 (6H, s, CH_2), 1.7 (6H, s, CH_2).

Compounds **4**−**10** were prepared based upon a literature bioconjugation method[62] from a solution of DMF (10 mL) containing AdA, AdA_{OH}, AdA_{dMe}, AdAc, MPOAc, L_{1D}, or **3** (1 mmol), EDC (1.5 mmol), **1** (1 mmol), and HOBt (0.19 g, 1.5 mmol), which was heated to 45 °C. After the reagents had dissolved, DIPEA (2 mmol) was added to the solution and the mixture was stirred overnight at room temperature under nitrogen. The solution was evaporated to dryness in vacuo and the solid residue was washed with diethylether (3 mL) and distilled water (3 mL) before redissolving the solid in methanol and removing the solvent under reduced pressure. The progress of all syntheses was monitored using TLC. Compounds **4**−**10** were not sufficiently soluble in water or methanol to enable purification using either recrystallization or flash chromatography and were, therefore, purified to >95% purity, using preparative RP-HPLC. This level of purity was confirmed by CHN microanalysis.

DFOB-AdA (4). The residue was triturated with diethylether (5 × 5 mL), recrystallized from methanol and purified by preparative RP-HPLC (90:10 (A:B) to 25:75 (A:B) over 30 min) to give **4** as a off-white solid (0.56 g, 70%). Solubility in ethanol (25 °C): 28 mg mL^{-1} (~38 mM). ^{1}H NMR (300 MHz, DMSO-d_6) δ_H: 9.6 (2H, m, NH), 7.7 (3H, s, OH), 7.3 (1H, s, NH), 3.4 (6H, t, J = 9 Hz, CH_2), 3.0 (4H, q, J = 6 Hz, CH_2), 2.6 (4H, t, J = 6 Hz, CH_2), 2.3 (4H, t, J = 6 Hz, CH_2), 1.9 (3H, s, CH_3), 1.7 (3H, s, CH), 1.6 (12H, m, CH_2), 1.1−1.5 (18H, m, CH_2). ^{13}C NMR (300 MHz, DMSO-d_6) δ_C: 177.1, 172.3, 171.6, 47.5, 47.2, 36.5, 30.3, 29.2, 28.0, 27.9, 26.4, 23.9, 23.8, 20.7. MS: *m*/*z* ESI (positive ion). Found $[M + H^+]^+$ 723.07 (98), $[M + Na^+]^+$ 745.27 (100), $[C_{36}H_{62}N_6O_9Na]^+$ requires 745.91. MeOH (320 nm), ε = 18.27 M^{-1} cm^{-1}. Anal. Calcd for $C_{36}H_{62}N_6O_9$: C, 59.81% H; 8.64%; N, 11.63%. Found: C, 57.44% H; 7.50%; N, 11.15%.

DFOB-AdA_{OH} (5). The residue was triturated with diethylether (5 × 5 mL), recrystallized from methanol and purified by RP-HPLC (90:10 (A:B) to 25:75 (A:B) over 30 min) to give **5** as

an off-white solid (0.45 g, 61%). Solubility in ethanol (25 °C): 15.2 mg mL^{-1} (~20 mM). Solubility in water (25 °C): 5 mg mL^{-1} (~6.5 mM). ^{1}H NMR (300 MHz, DMSO-d_6) δ_H: 9.6 (2H, m, NH), 7.7 (3H, s, OH), 7.3 (1H, s, NH), 3.4 (6H, t, J = 9 Hz, CH_2), 3.2 (1H, s, OH), 3.0 (4H, q, J = 6 Hz, CH_2), 2.6 (4H, t, J = 6 Hz, CH_2), 2.3 (4H, t, J = 6 Hz, CH_2), 1.9 (3H, s, CH_3), 1.7 (2H, s, CH), 1.5−1.6 (12H, m, CH_2), 1.2−1.5 (18H, m, CH_2). ^{13}C NMR (300 MHz, DMSO-d_6) δ_C: 176.3, 171.7, 67.0, 56.4, 47.2, 44.7, 38.2, 31.0, 30.3, 29.2, 27.9, 26.4, 23.9, 23.8, 20.7. MS: m/z ESI (positive ion). Found $[M + H^+]^+$ 737.20 (100), $[C_{36}H_{63}N_6O_{10}]^+$ requires 739.92. MeOH (320 nm), ε = 49.74 M^{-1} cm^{-1}. Anal. Calcd for $C_{36}H_{62}N_6O_{10}$: C, 58.51% H; 8.46%; N, 11.38%. Found: C, 56.88% H; 8.21%; N, 10.92%.

DFOB-AdA$_{dMe}$ (6). The residue was triturated with diethylether (5 × 5 mL), recrystallized from methanol, and purified by RP-HPLC (90:10 (A:B) to 40:60 (A:B) over 30 min) to give **6** as an off-white solid (0.57 g, 80%). Solubility in ethanol (25 °C): 15 mg mL^{-1} (~20 mM). ^{1}H NMR (300 MHz, DMSO-d_6) δ_H: 9.6 (2H, m, NH), 7.7 (3H, s, OH), 7.3 (1H, s, NH), 3.4 (6H, t, J = 15 Hz, CH_2), 3.0 (4H, q, J = 6 Hz, CH_2), 2.6 (4H, t, J = 9 Hz, CH_2), 2.3 (4H, t, J = 6 Hz, CH_2), 1.9 (3H, s, CH_3), 1.6−1.1 (31H, m, CH_2, CH), 0.8 (6H, s, CH_3). ^{13}C NMR (300 MHz, d_6-DMSO) δ_C: 176.8, 172.3, 171.7, 50.7, 45.4, 42.8, 37.8, 31.1, 28.2, 27.9, 26.4, 23.9, 23.8, 20.7. MS: m/z ESI (positive ion). Found $[M + H^+]^+$ 751.13 (100), $[C_{38}H_{67}N_6O_9]^+$ requires 751.98. MeOH (320 nm), ε = 32.17 M^{-1} cm^{-1}. Anal. Calcd for $C_{38}H_{66}N_6O_9$: C, 60.77% H; 8.86%; N, 11.19%. Found: C, 58.85% H; 8.04%; N, 10.71%.

DFOB-AdAc (7). The residue was triturated with diethylether (5 × 5 mL), recrystallized from methanol, and purified by RP-HPLC (90:10 (A:B) to 25:75 (A:B) over 30 min) to give **7** as an off-white solid (0.55 g, 80%). Solubility in ethanol (25 °C): 15 mg mL^{-1} (~20 mM). ^{1}H NMR (300 MHz, DMSO-d_6) δ_H: 9.6 (2H, m, NH), 7.7 (3H, s, OH), 7.3 (1H, s, NH), 3.4 (6H, t, J = 6 Hz, CH_2), 3.0 (4H, q, J = 6 Hz, CH_2), 2.6 (4H, t, J = 6 Hz, CH_2), 2.3 (4H, t, J = 6 Hz, CH_2), 1.9 (3H, s, CH_3), 1.8 (2H, s, CH_2), 1.7 (3H, s, CH), 1.5−1.6 (12H, m, CH_2), 1.0−1.5 (18H, m, CH_2). ^{13}C NMR (300 MHz, d_6-DMSO) δ_C: 171.6, 170.1, 50.4, 42.5, 36.8, 30.2, 29.2, 28.4, 27.9, 26.4, 23.9, 20.7. MS: m/z ESI (positive ion). Found $[M + H^+]^+$ 737.44 (100), $[C_{37}H_{65}N_6O_9]^+$ requires 737.95. MeOH (320 nm), ε = 16.53 M^{-1} cm^{-1}. Anal. Calcd for $C_{37}H_{64}N_6O_9$: C, 60.30% H; 8.75%; N, 11.41%. Found: C, 58.37% H; 8.53%; N, 11.72%.

DFOB-MPOAc (8). The residue was triturated with diethylether (5 × 5 mL), recrystallized from methanol, and purified by RP-HPLC (90:10 (A:B) to 40:60 (A:B) over 30 min) to give **8** as an off-white solid (0.23 g, 73%). ^{1}H NMR (200 MHz, DMSO-d_6) δ_H: 7.1 (2H, d, J = 7.1 Hz, CH), 6.8 (2H, d, J = 7.0 Hz, CH), 4.4 (2H, s, CH_2), 3.5 (6H, t, J = 6.8 Hz, CH_2), 3.0 (4H, m, CH_2), 2.5 (4H, m, CH_2), 2.3 (4H, m, CH_2), 2.2 (3H, s, CH_3), 1.9 (3H, s, CH_3), 1.3−1.5 (12H, m, CH_2), 1.2 (6H, m, CH_2). ^{13}C NMR (200 MHz, DMSO-d_6) δ_C: 21.1, 21.4, 24.5, 27.1, 28.5, 29.8, 31.0, 47.8, 48.2, 68.2, 115.6, 130.8, 156.7, 168.6, 172.3, 173.0. MS: m/z ESI (positive ion). Found $[M + Na^+]^+$ 731.7 (100), $[C_{34}H_{56}N_6O_{10}Na]^+$ requires 731.40. MeOH (320 nm), ε = 101.63 M^{-1} cm^{-1}. Anal. Calcd for $C_{34}H_{56}N_6O_{10}$: C, 57.61% H; 7.96%; N, 11.86%. Found: C, 56.60% H; 7.31%; N, 11.73%.

DFOB-L$_{1D}$ (9). The residue was triturated with diethylether (5 × 5 mL), recrystallized from methanol, and purified by RP-HPLC (95:5 (A:B) to 40:60 (A:B) over 30 min) to give **9** as a very pale-pink solid (0.11 g, 70%). ^{1}H NMR (300 MHz, CD_3OD) δ_H: 8.2 (1H, d, J = 7.0 Hz, CH), 7.2 (1H, d, J = 7.0 Hz, CH), 5.2 (2H, s, CH_2), 3.6 (6H, t, J = 5.6 Hz, CH_2), 3.2 (4H, t, J = 6.9 Hz, CH_2), 2.8 (4H, t, J = 6.8 Hz, CH_2), 2.5 (4H, t, J = 7.0 Hz, CH_2), 2.1 (3H, s, CH_3), 1.5−1.7 (12H, m, CH_2), 1.3−1.4 (6H, m, CH_2), (OH not observed). ^{13}C NMR (300 MHz, CD_3OD) δ_C: 19.2, 23.9, 26.2, 26.3, 27.9, 28.8, 28.9, 30.4, 39.3, 39.7, 48.9, 58.0, 113.1, 139.8, 142.8, 143.9, 159.7, 165.6, 172.5, 173.5, 173.9. MS: m/z ESI (positive ion). Found $[M + H^+]^+$ 726.6 (65), $[M + Na^+]^+$ 748.7 (100), $[C_{46}H_{61}N_9O_{11}Na]^+$ requires 748.8. MeOH (320 nm), ε = 99.6 M^{-1} cm^{-1}. Anal. Calcd for $C_{33}H_{55}N_7O_{11}\cdot 2H_2O$: C, 52.02% H; 7.81%; N, 12.87%. Found: C, 49.69% H; 6.42%; N, 11.93%.

DFOB-L$_{DX}$ (10). The residue was triturated with diethylether (5 × 5 mL), recrystallized from methanol, and purified by RP-HPLC (95:5 (A:B) to 45:55 (A:B) over 30 min) to give **10** as an off-white solid (0.14 g, 65%). ^{1}H NMR (200 MHz, CD_3OD) δ_H: 8.2 (2H, d, J = 6.9 Hz, CH), 7.9 (2H, d, J = 6.5 Hz, CH), 7.6 (2H, d, J = 6.8 Hz, CH), 7.4 (2H, m, CH), 6.9−7.0 (4H, m, CH), 3.6 (6H, t, J = 6.8 Hz, CH_2), 3.2 (4H, m, CH_2), 2.8 (4H, m, CH_2), 2.4 (4H, m, CH_2), 2.1 (3H, s, CH_3), 1.6−1.7 (8H, m, CH_2), 1.5 (4H, m, CH_2), 1.3 (6H, m, CH_2), (OH not observed). ^{13}C NMR (200 MHz, CD_3OD) δ_C: 19.2, 23.7, 23.9, 26.3, 27.9, 29.0, 30.5, 39.2, 39.9, 44.7, 116.3, 119.6, 119.8, 123.8, 127.2, 128.3, 130.9, 131.4, 133.5, 141.5, 157.2, 160.1, 173.2, 173.5. MS: m/z ESI (positive ion). Found $[M + H^+]^+$ 916.5 (85), $[M + Na^+]^+$ 938.7 (100), $[C_{46}H_{61}N_9O_{11}Na]^+$ requires 939.03. MeOH (320 nm), ε = 3.127 × 10^3 M^{-1} cm^{-1}. Anal. Calcd for $C_{46}H_{61}N_9O_{11}$: C, 60.31% H; 6.91%; N, 13.76%. Found: C, 59.40% H; 5.63%; N, 13.38%.

Extinction Coefficients and Job's Plot Analysis. A plot of absorbance/path length (cm^{-1}) at 320 nm vs concentration (M) in methanol of **4**−**10** was measured using a SpectraMax M5/M5^e UV−vis (Molecular Devices, Sunnyvale, CA) and the slope of the line determined as ε (M^{-1} cm^{-1}). Job's Plots analyses were carried out for **4**−**10**, as detailed in the literature,[85] with compounds (0.1 mM) dissolved in a solution of 20% (v/v) MeOH in Tris·HCl (100 mM, pH 7.4) and the pH value of the solution adjusted to pH 7.4 prior to making the solution to volume. A stock solution of Fe(III) (0.1 mM) was prepared from $FeCl_3\cdot 6H_2O$ in a similar fashion to the compounds (20% v/v MeOH in 100 mM Tris, pH 7.4). Molar ratios of Fe:compound were 0, 0.1, 0.2, 0.3, 0.4, 0.5, 0.6, 0.7, 0.8, 0.9, and 1, with 0 containing no iron and 1 containing no ligand. All samples had a final concentration ([Fe(III)] + [ligand]) of 0.1 mM and electronic absorption spectra were acquired from 200 to 800 nm, with the absorbance value of 450 nm absorbance used to construct the Job's plot.

Fe(III)-Loading of 4−10 for ESI-MS and RP-HPLC. An aliquot of a freshly prepared methanolic solution of $FeCl_3\cdot 6H_2O$ (100 μL of 10 mM) was added to an aliquot (100 μL of 10 mM) of **4**−**8** in methanol. For **9** and **10**, the volume ratio of $FeCl_3\cdot 6H_2O$:compound was 150:50 μL.

Partition Coefficients. Analytical RP-HPLC was used to estimate the log of the partition coefficients (log$P$) of **4**−**10**. Samples (5 mM) of **4**−**10** in MeOH (HPLC grade) were filtered (0.22 μm) and analyzed by analytical RP-HPLC, together with a set of compounds with known log$P$ values (1,2-benzenedicarboxylic acid dimethylester (log$P$ = 1.59), 1,2-benzenedicarboxylic acid diethylester (log$P$ = 2.48), naphthalene (log$P$ = 3.27), and dibenzofuran (log$P$ = 3.76)). The capacity factor (k) was determined for the samples using eq 1, where t_r was the retention time of the compound and t_o was the deadtime (t_o = 1.81 min). The log of the partition coefficient (log$P$) was calculated according to eq 2.[76]

$$k = (t_r - t_o)/t_o \quad (1)$$

$$\log k = a + b\log P \quad (2)$$

Partition coefficients were also determined using the shake-flask method with presaturated 1-octanol and water solutions as follows. An aliquot (1 mL) of water was added to an aliquot of 1-octanol containing dissolved **4**−**10** (1 or 2 mg) in a glass vial, and the mixture was shaken overnight at RT. Aliquots (20 μL) of each phase were analyzed by analytical RP-HPLC using the conditions described above.

Molecular Modeling. Models were built in HyperChem 7.5 using data from X-ray crystal structures of $[Fe(\mathbf{1}(3-))]^+$,[17] 2,5-dioxopyrrolidin-1-yl adamantane-1-carboxylate,[61] $[Cr(\mathbf{2}(1-))_3]$,[73] and $[Fe\{(3,5\text{-bis}(2\text{-hydroxyphenyl})\text{-}1\text{-phenyl-}1,2,4\text{-triazole})(2-)\}_2]$.[69] The structure of the organic ancillary fragment was minimized

using the Polak-Ribiere algorithm and the MM+ force field and the structure of the Fe(III)-loaded ligand was frozen. No conformational searching procedure was used.

Biological Studies. Cell Culture. The human SK-N-MC neuroepithelioma and Madin−Darby canine kidney type II (MDCK II) cell lines were obtained from the American Type Culture Collection (ATCC; Manassas, VA). The SK-N-MC cell type was grown as described previously,[77] while MDCK II cells were cultured by standard procedures.[86]

^{59}Fe-Transferrin Labeling. Human transferrin (Tf) was labeled with ^{59}Fe (Dupont NEN, MA) to produced $^{59}Fe_2$-Tf (^{59}Fe-Tf), as previously described.[87,88]

^{59}Fe Efflux from SK-N-MC Neuroepithelioma Cells. Efflux of ^{59}Fe from SK-N-MC neuroepithelioma cells were measured for **1**−**10** and for Dp44mT at concentrations of 50 μM using established techniques.[38,77,89] Briefly, following prelabeling of cells with ^{59}Fe-Tf (0.75 μM) for 3 h at 37 °C, the cell cultures were washed four times with ice-cold PBS and then subsequently incubated with each chelator (50 μM) for 3 h at 37 °C. The overlying media containing released ^{59}Fe was then separated from the cells using a Pasteur pipet. Radioactivity was measured in both the cell pellet and supernatant using a γ-scintillation counter (Wallac Wizard 3, Turku, Finland). In these studies, the new ligands were compared to the previously characterized chelators, **1**, **2**, **3**, and Dp44mT.

Effect of 1−10 at Preventing ^{59}Fe Uptake from Transferrin by SK-N-MC Neuroepithelioma Cells. The uptake of ^{59}Fe from ^{59}Fe-labeled transferrin was measured for **1**−**10** and for Dp44mT at concentrations of 50 μM in SK-N-MC neuroepithelioma cells using standard techniques.[38,77,89] Briefly, cells were incubated with ^{59}Fe-Tf (0.75 μM) for 3 h at 37 °C in the presence of each of the chelators (50 μM). The cells were then washed four times with ice-cold PBS and internalized ^{59}Fe was determined by standard techniques by incubating the cell monolayer for 30 min at 4 °C with the general protease Pronase (1 mg/mL; Sigma).[87,88] The cells were removed from the monolayer using a plastic spatula and centrifuged for 1 min at 14000 rpm. The supernatant represents membrane-bound, Pronase-sensitive ^{59}Fe that was released by the protease, while the Pronase-insensitive fraction represents internalized ^{59}Fe. The new ligands were compared to the previously characterized chelators, **1**, **2**, **3**, and Dp44mT.

Effect of 1−10 on Cell Viability. This was examined in Madin−Darby canine kidney type II (MDCK II) cells and in human SK-N-MC neuroepithelioma cells using the MTT assay by standard methods.[77,82,90] MTT color formation was directly proportional to the number of viable cells measured by Trypan blue staining (SK-N-MC)[77] or total cell protein (MDCK II).[86]

Statistical Analysis. Experimental data were compared using Student's *t*-test. Results were expressed as mean or mean ± SD (number of experiments) and considered to be statistically significant when $p < 0.05$.

Acknowledgment. This work was supported by the National Health and Medical Research Council of Australia (grant to RC; Senior Principal Research Fellowship and Project grants to DRR), the Australian Research Council (Discovery grants to DRR and PKW), and The University of Sydney (Faculty of Medicine Strategic Research grant to RC, Sydnovate Fund grant to RC; Faculty of Medicine cofunded postgraduate scholarship to JL). DSK was supported by a Cancer Institute New South Wales Early Career Development Fellowship. Microanalysis was performed at the Chemical Analysis Facility at Macquarie University, Sydney, Australia.

References

(1) Weatherall, D.; Akinyanju, O.; Fucharoen, S.; Olivieri, N.; Musgrove, P. Inherited Disorders of Hemoglobin. In *Disease Control Priorities in Developing Countries*, 2nd ed.; Jamison, D. T., Breman, J. G., Measham, A. R., Alleyne, G., Claeson, M., Evans, D. B., Jha, P., Mills, A., Musgrove, P., Eds.; Oxford University Press: New York, 2006; pp 663−680.

(2) Weatherall, D. J.; Clegg, J. B. Inherited Haemoglobin Disorders: An Increasing Global Health Problem. *Bull. WHO* **2001**, *79*, 704–712.

(3) Nick, H. Iron Chelation, Quo Vadis? *Curr. Opin. Chem. Biol.* **2007**, *11*, 419–423.

(4) Hershko, C.; Link, G.; Konijn, A. M. Iron Chelation. In *Molecular and Cellular Iron Transport*; Templeton, D. M., Ed.; Marcel Dekker, Inc.: New York, 2002; pp 787−816.

(5) Barton, J. C. Chelation Therapy for Iron Overload. *Curr. Gastroenterol. Rep.* **2007**, *9*, 74–82.

(6) Bernhardt, P. V. Coordination Chemistry and Biology of Chelators for the Treatment of Iron Overload Disorders. *Dalton Trans.* **2007**, 3214–3220.

(7) Kalinowski, D. S.; Richardson, D. R. The Evolution of Iron Chelators for the Treatment of Iron Overload Disease and Cancer. *Pharmacol. Rev.* **2005**, *57*, 547–583.

(8) Bickel, H.; Bosshardt, R.; Gäumann, E.; Reusser, P.; Vischer, E.; Voser, W.; Wettstein, A.; Zähner, H. Metabolic Products of Actinomycetaceae. XXVI. Isolation and Properties of Ferrioxamines A to F, Representing New Sideramine Compounds. *Helv. Chim. Acta* **1960**, *43*, 2118–2128.

(9) Stintzi, A.; Barnes, C.; Xu, J.; Raymond, K. N. Microbial Iron Transport via a Siderophore Shuttle: A Membrane Ion Transport Paradigm. *Proc. Natl. Acad. Sci. U.S.A.* **2000**, *97*, 10691–10696.

(10) Butler, A. Marine Siderophores and Microbial Iron Mobilization. *BioMetals* **2005**, *18*, 369–374.

(11) Drechsel, H.; Winkelmann, G. Iron Chelation and Siderophores. In *Transition Metals in Microbial Metabolism*; Winkelmann, G., Carrano, C. J., Eds.; Harwood Academic: Amsterdam, 1997; pp 1−49.

(12) Braich, N.; Codd, R. Immobilized Metal Affinity Chromatography for the Capture of Hydroxamate-Containing Siderophores and Other Fe(III)-binding Metabolites from Bacterial Culture Supernatants. *Analyst* **2008**, *133*, 877–880.

(13) Porter, J. B.; Rafique, R.; Srichairatanakool, S.; Davis, B. A.; Shah, F. T.; Hair, T.; Evans, P. Recent Insights into Interactions of Deferoxamine with Cellular and Plasma Iron Pools: Implications for Clinical Use. *Ann. N.Y. Acad. Sci.* **2005**, *1054*, 155–168.

(14) Glickstein, H.; Ben El, R.; Link, G.; Breuer, W.; Konjin, A. M.; Hershko, C.; Nick, H.; Cabantchik, Z. Action of Chelators in Iron-Loaded Cardiac Cells: Accessibility to Intracellular Labile Iron and Functional Consequences. *Blood* **2006**, *108*, 3195–3203.

(15) Olivieri, N. F.; Brittenham, G. M. Iron-Chelating Therapy and the Treatment of Thalassemia. *Blood* **1997**, *89*, 739–761.

(16) Konetschny-Rapp, S.; Jung, G.; Raymond, K. N.; Meiwes, J.; Zaehner, H. Solution Thermodynamics of The Ferric Complexes of New Desferrioxamine Siderophores Obtained by Directed Fermentation. *J. Am. Chem. Soc.* **1992**, *114*, 2224–2230.

(17) Dhungana, S.; White, P. S.; Crumbliss, A. L. Crystal Structure of Ferrioxamine B: A Comparative Analysis and Implications for Molecular Recognition. *J. Biol. Inorg. Chem.* **2001**, *6*, 810–818.

(18) Codd, R. Traversing the Coordination Chemistry and Chemical Biology of Hydroxamic Acids. *Coord. Chem. Rev.* **2008**, *252*, 1387–1408.

(19) Cappellini, M. D.; Pattoneri, P. Oral Iron Chelators. *Annu. Rev. Med.* **2009**, *60*, 25–38.

(20) Scott, L. E.; Orvig, C. Medicinal Inorganic Chemistry Approaches to Passivation and Removal of Aberrant Metal Ions in Disease. *Chem. Rev.* **2009**, *109*, 4885–4910.

(21) Kontoghiorghes, G. J.; Pattichis, K.; Neocleous, K.; Kolnagou, A. The Design and Development of Deferiprone (L1) and Other Iron Chelators for Clinical Use: Targeting Methods and Application Prospects. *Curr. Med. Chem.* **2004**, *11*, 2161–2183.

(22) Olivieri, N. F.; Brittenham, G. M.; McLaren, C. E.; Templeton, D. M.; Cameron, R. G.; McClelland, R. A.; Burt, A. D.; Fleming, K. A. Long-Term Safety and Effectiveness of Iron-Chelation Therapy with Deferiprone for Thalassemia Major. *N. Engl. J. Med.* **1998**, *339*, 417–423.

(23) Hoffbrand, A. V.; Al-Refaie, F.; Davis, B.; Siritanakatkul, N.; Jackson, B. F. A.; Cochrane, J.; Prescott, E.; Wonke, B. Long-term Trial of Deferiprone in 51 Transfusion-Dependent Iron Overloaded Patients. *Blood* **1998**, *91*, 295–300.

(24) Hershko, C. Oral Iron Chelators: New Opportunities and New Dilemmas. *Haematologica* **2006**, *91*, 1307–1312.

(25) Hershko, C.; Konijn, A. M.; Nick, H. P.; Breuer, W.; Cabantchik, Z. I.; Link, G. ICL670A: A New Synthetic Oral Chelator: Evaluation in Hypertransfused Rats with Selective Radioiron Probes of Hepatocellular and Reticuloendothelial Iron Stores and in Iron-Loaded Rat Heart Cells in Culture. *Blood* **2001**, *97*, 1115–1122.

(26) Bergeron, R. J.; Streiff, R. R.; Creary, E. A.; Daniels, R. D., Jr.; King, W.; Luchetta, G.; Wiegand, J.; Moerker, T.; Peter, H. H. A. A Comparative Study of the Iron-Clearing Properties of Desferrithiocin Analogues with Desferrioxamine B in a *Cebus* Monkey Model. *Blood* **1993**, *81*, 2166–2173.
(27) Bergeron, R. J.; Wiegand, J.; McManis, J. S.; Vinson, J. R. T.; Yao, H.; Bharti, N.; Rocca, J. R. (*S*)-4,5-Dihydro-2-(2-hydroxy-4-hydroxyphenyl)-4-methyl-4-thiazolecarboxylic Acid Polyethers: A Solution to Nephrotoxicity. *J. Med. Chem.* **2006**, *49*, 2772–2783.
(28) Donovan, J. M.; Plone, M.; Dagher, R.; Bree, M.; Marquis, J. Preclinical and Clinical Development of Deferitrin, A Novel, Orally Available Iron Chelator. *Ann. N.Y. Acad. Sci.* **2005**, *1054*, 492–494.
(29) Brosnahan, G.; Gokden, N.; Swaminathan, S. Acute Interstitial Nephritis due to Deferasirox: A Case Report. *Nephrol. Dial. Transplant.* **2008**, *23*, 3356–3358.
(30) Kontoghiorghes, G. J. Deferasirox: Uncertain Future Following Renal Failure Fatalities, Agranulocytosis and Other Toxicities. *Expert Opin. Drug Saf.* **2007**, *6*, 235–239.
(31) Turcot, I.; Stintzi, A.; Xu, J.; Raymond, K. N. Fast Biological Iron Chelators: Kinetics of Iron Removal from Human Diferric Transferrin by Multidentate Hydroxypyridonate. *J. Biol. Inorg. Chem.* **2000**, *5*, 634–641.
(32) Kalinowski, D. S.; Richardson, D. R. Future of Toxicology−Iron Chelators and Differing Modes of Action and Toxicity: The Changing Face of Iron Chelation Therapy. *Chem. Res. Toxicol.* **2007**, *20*, 715–720.
(33) Kalinowski, D. S.; Sharpe, P. C.; Bernhardt, P. V.; Richardson, D. R. Structure−Activity Relationships of Novel Iron Chelators for the Treatment of Iron Overload Disease: The Methyl Pyrazinylketone Isonicotinoyl Hydrazone Series. *J. Med. Chem.* **2008**, *51*, 331–344.
(34) Bernhardt, P. V.; Chin, P.; Sharpe, P. C.; Richardson, D. R. Hydrazone Chelators for the Treatment of Iron Overload Disorders: Iron Coordination Chemistry and Biological Activity. *Dalton Trans.* **2007**, 3232–3244.
(35) Bernhardt, P. V.; Wilson, G. J.; Sharpe, P. C.; Kalinowski, D. S.; Richardson, D. R. Tuning the Antiproliferative Activity of Biologically Active Iron Chelators: Characterization of the Coordination Chemistry and Biological Efficacy of 2-Acetylpyridine and 2-Benzoylpyridine Hydrazone Ligands. *J. Biol. Inorg. Chem.* **2008**, *13*, 107–119.
(36) Richardson, D. R.; Sharpe, P. C.; Lovejoy, D. B.; Senaratne, D.; Kalinowski, D. S.; Islam, M.; Bernhardt, P. V. Dipyridyl Thiosemicarbazone Chelators with Potent and Selective Antitumor Activity Form Iron Complexes with Redox Activity. *J. Med. Chem.* **2006**, *49*, 6510–6521.
(37) Bernhardt, P. V.; Sharpe, P. C.; Islam, M.; Lovejoy, D. B.; Kalinowski, D. S.; Richardson, D. R. Iron Chelators of the Dipyridylketone Thiosemicarbazone Class: Precomplexation and Transmetalation Effects on Anticancer Activity. *J. Med. Chem.* **2009**, *52*, 407–415.
(38) Kalinowski, D. S.; Sharpe, P. C.; Bernhardt, P. V.; Richardson, D. R. Design, Synthesis, and Characterization of New Iron Chelators with Anti-Proliferative Activity: Structure−Activity Relationships of Novel Thiohydrazone Analogues. *J. Med. Chem.* **2007**, *50*, 6212–6225.
(39) Richardson, D. R.; Kalinowski, D. S.; Richardson, V.; Sharpe, P. C.; Lovejoy, D. B.; Islam, M.; Bernhardt, P. V. 2-Acetylpyridine Thiosemicarbazones are Potent Iron Chelators and Antiproliferatuve Agents: Redox Activity, Iron Complexation and Characterization of their Antitumor Activity. *J. Med. Chem.* **2009**, *52*, 1459–1470.
(40) Whitnall, M.; Howard, J. B.; Ponka, P.; Richardson, D. R. A Class of Iron Chelators with a Wide Spectrum of Potent Antitumor Activity that Overcomes Resistance to Chemotherapeutics. *Proc. Natl. Acad. Sci. U.S.A.* **2006**, *103*, 14901–14906.
(41) Loyevsky, M.; Lytton, S. D.; Mester, B.; Libman, J.; Shanzer, A.; Cabantchik, Z. I. The Antimalarial Action of Desferal Involves a Direct Access Route to Erythrocytic (*Plasmodium falciparum*) Parasites. *J. Clin. Invest.* **1993**, *91*, 218–224.
(42) Palanché, T.; Marmolle, F.; Abdallah, M. A.; Shanzer, A.; Albrecht-Gary, A.-M. Fluorescent Siderophore-Based Chemosensors: Iron(III) Quantitiative Determinations. *J. Biol. Inorg. Chem.* **1999**, *4*, 188–198.
(43) Ghosh, M.; Lambert, L. J.; Huber, P. W.; Miller, M. J. Synthesis, Bioactivity, and DNA-Cleaving Ability of Desferrioxamine B-Nalidixic Acid and Anthraquinone Carboxylic Acid Conjugates. *Bioorg. Med. Chem. Lett.* **1995**, *5*, 2337–2340.
(44) Diarra, M. S.; Lavoie, M. C.; Jacques, M.; Darwish, I.; Dolence, E. K.; Dolence, J. A.; Ghosh, A.; Ghosh, M.; Miller, M. J.; Malouin, F. Species Selectivity of New Siderophore-Drug Conjugates that use Specific Iron Uptake for Entry into Bacteria. *Antimicrob. Agents Chemother.* **1996**, *40*, 2610–2617.
(45) Moggia, F.; Brisset, H.; Fages, F.; Chaix, C.; Mandrand, B.; Dias, M.; Levillain, E. Design, Synthesis and Redox Properties of Two Ferrocene-Containing Iron Chelators. *Tetrahedron Lett.* **2006**, *47*, 3371–3374.
(46) Hou, Z.; Whisenhunt, D. W. J.; Xu, J.; Raymond, K. N. Potentiometric, Spectrophotometric, and ^{1}H NMR Study or Four Desferrioxamine B Derivatives and Their Ferric Complexes. *J. Am. Chem. Soc.* **1994**, *116*, 840–846.
(47) Rodgers, S. J.; Raymond, K. N. Ferric Ion Sequestering Agents. 11. Synthesis and Kinetics of Iron Removal from Transferrin of Catechoyl Derivatives of Desferrioxamine B. *J. Med. Chem.* **1983**, *26*, 439–442.
(48) White, D. L.; Durbin, P. W.; Jeung, N.; Raymond, K. N. Specific Sequestering Agents from the Actinites. 16. Synthesis and Initial Biological Testing of Polydentate Oxohydroxypyridinecarboxylate Ligands. *J. Med. Chem.* **1988**, *31*, 11–18.
(49) Laub, R.; Schneider, Y. J.; Octave, J. N.; Trouet, A.; Crichton, R. R. Cellular Pharmacology of Deferrioxamine B and Derivatives in Cultured Rat Hepatocytes in Relation to Iron Mobilization. *Biochem. Pharmacol.* **1985**, *34*, 1175–1183.
(50) Rosebrough, S. F. Plasma Stability and Pharmacokinetics of Radiolabeled Deferoxamine-Biotin Derivatives. *J. Pharmacol. Exp. Ther.* **1993**, *265*, 408–415.
(51) Ihnat, P. M.; Vennerstrom, J. L.; Robinson, D. H. Synthesis and Solution Properties of Deferoxamine Amides. *J. Pharmaceut. Sci.* **2000**, *89*, 1525–1536.
(52) Hallaway, P. E.; Eaton, J. W.; Panter, S. S.; Hedlund, B. E. Modulation of Deferoxamine Toxicity and Clearance by Covalent Attachment to Biocompatible Polymers. *Proc. Natl. Acad. Sci. U.S.A.* **1989**, *86*, 10108–10112.
(53) Miller, M. J.; Zhu, H.; Xu, Y.; Wu, C.; Walz, A. J.; Vergne, A.; Roosenberg, J. M.; Moraski, G.; Minnick, A. A.; McKee-Dolence, J.; Hu, J.; Fennell, K.; Dolence, E. K.; Dong, L.; Franzblau, S.; Malouin, F.; Mollmann, U. Utilization of Microbial Iron Assimilation Processes for the Development of New Antibiotics and Inspiration for the Design of New Anticancer Agents. *BioMetals* **2009**, *22*, 61–75.
(54) Roosenberg, J. M. I.; Lin, Y.-M.; Lu, Y.; Miller, M. J. Studies and Syntheses of Siderophores, Microbial Iron Chelators, and Analogs as Potential Drug Delivery Agents. *Curr. Med. Chem.* **2000**, *7*, 159–197.
(55) Stouffer, A. L.; Acharya, R.; Salom, D.; Levine, A. S.; Di Costanzo, L.; Soto, C. S.; Tereshko, V.; Nanda, V.; Stayrook, S.; De Grado, W. F. Structural Basis for the Function and Inhibition of an Influenza Virus Proton Channel. *Nature* **2008**, *451*, 596–599.
(56) Moresco, R. M.; Volonte, M. A.; Messa, C.; Gobbo, C.; Galli, L.; Carpinelli, A.; Rizzo, G.; Panzacchi, A.; Franceschi, M.; Fazio, F. New Perspectives on Neurochemical Effects of Amantadine in the Brain of Parkinsonian Patients: A PET−[^{11}C]Raclopride Study. *J. Neural Transm.* **2002**, *109*, 1265–1274.
(57) De Felice, F. G.; Velasco, P. T.; Lambert, M. P.; Viola, K.; Fernandez, S. J.; Ferreira, S. T.; Klein, W. L. Aβ Oligomers Induce Neuronal Oxidative Stress through an *N*-Methyl-D-aspartate Receptor-dependent Mechanism That Is Blocked by the Alzheimer Drug Memantine. *J. Biol. Chem.* **2007**, *282*, 11590–11601.
(58) Jia, L.; Tomaszewski, J. E.; Hanrahan, C.; Coward, L.; Noker, P.; Gorman, G.; Nikonenko, B.; Protopopova, M. Pharmacodynamics and Pharmacokinetics of SQ109, a New Diamine-Based Antitubercular Drug. *Br. J. Pharmacol.* **2005**, *144*, 80–87.
(59) Zhang, Z.; Rettig, S. J.; Orvig, C. Physical and Structural Studies of *N*-Carboxymethyl- and *N*-(*p*-Methoxyphenyl)-3-hydroxy-2-methyl-4-pyridinone. *Can. J. Chem.* **1992**, *70*, 763–770.
(60) Kruck, T. P. A.; Burrow, T. E. Synthesis of Feralex A Novel Aluminum/Iron Chelating Compound. *J. Inorg. Biochem.* **2002**, *88*, 19–24.
(61) Liu, J.; Clegg, J. K.; Codd, R. 2,5-Dioxopyrrolidin-1-yl Adamantane-1-carboxylate. *Acta Crystallogr., Sect. E: Struct. Rep. Online* **2009**, *65*, o1740–o1741.
(62) Lau, J.; Behrens, C.; Sidelmann, U. G.; Knudsen, L. B.; Lundt, B.; Sams, C.; Ynddal, L.; Brand, C. L.; Pridal, L.; Ling, A.; Kiel, D.; Plewe, M.; Shi, S.; Madsen, P. New β-Alanine Derivatives are Orally Available Glucagon Receptor Antagonists. *J. Med. Chem.* **2007**, *50*, 113–128.
(63) Boukhalfa, H.; Reilly, S. D.; Neu, M. P. Complexation of Pu(IV) with the Natural Siderophore Desferrioxamine B and the Redox Properties of Pu(IV)(siderophore) Complexes. *Inorg. Chem.* **2007**, *46*, 1018–1026.
(64) Sinha, A.; Lopez, L. P. H.; Schrock, R. R.; Hock, A. S.; Müller, P. Reactions of M(*N*-2−6-*i*-$Pr_2C_6H_3$)(CHR)$(CH_2R')_2$ (M = Mo, W) Complexes with Alcohols To Give Olefin Metathesis Catalysts of

the Type M(*N*-2,6-*i*-$Pr_2C_6H_3$)(CHR)(CH2R')(OR''). *Organometallics* **2006**, *25*, 1412–1423.
(65) Clarke, E. T.; Martell, A. E. Stabilities of 1,2-Dimethyl-3-hydroxy-4-pyridinone Chelates of Divalent and Trivalent Metal Ions. *Inorg. Chim. Acta* **1992**, *191*, 57–63.
(66) Santos, M. A.; Gama, S.; Pessoa, J. C.; Oliveira, M. C.; Toth, I.; Farkas, E. Complexation of Molybdenum(VI) with Bis(3-hydroxy-4-pyridinone)amino Acid Derivatives. *Eur. J. Inorg. Chem.* **2007**, 1728–1737.
(67) Heinz, U.; Hegetschweiler, K.; Acklin, P.; Faller, B.; Lattmann, R.; Schnebli, H. P. 4-[3,5-Bis(2-hydroxyphenyl)-1,2,4-triazole-1-yl]-benzoic Acid: A Novel Efficient and Selective Iron(III) Complexing Agent. *Angew. Chem., Int. Ed.* **1999**, *38*, 2568–2570.
(68) Devanur, L. D.; Neubert, H.; Hider, R. C. The Fenton Activity of Iron(III) in the Presence of Deferiprone. *J. Pharm. Sci.* **2008**, *97*, 1454–1467.
(69) Steinhauser, S.; Heinz, U.; Bartholomä, M.; Weyhermüller, T.; Nick, H.; Hegetschweiler, K. Complex Formation of ICL670 and Related Ligands with Fe^{III} and Fe^{II}. *Eur. J. Inorg. Chem.* **2004**, 4177–4192.
(70) Fontecave, M.; Pierre, J. L. Activation and Toxicity of Oxygen. 2. Iron and Hydrogen Peroxide: Biochemical Aspects. *Bull. Soc. Chim. Fr.* **1993**, *130*, 77–85.
(71) Spasojevic, I.; Armstrong, S. K.; Brickman, T. J.; Crumbliss, A. L. Electrochemical Behavior of the Fe(III) Complexes of the Cyclic Hydroxamate Siderophores Alcaligin and Desferrioxamine E. *Inorg. Chem.* **1999**, *38*, 449–454.
(72) Merkofer, M.; Kissner, R.; Hider, R. C.; Koppenol, W. H. Redox Properties of the Iron Complexes of Orally Active Iron Chelators CP20, CP502, CP509, and ICL670. *Helv. Chim. Acta* **2004**, *87*, 3021–3034.
(73) Hsieh, W.-Y.; Liu, S. Synthesis and Characterization of Cr(III) Complexes with 3-Hydroxy-4-Pyrones and 1,2-Dimethyl-3-Hydroxy-4-Pyridinone (DMHP): X-Ray Crystal Structures of $Cr(DMHP)_3 \cdot 12H_2O$ and $Cr(ma)_3$. *Synth. React. Inorg., Met.-Org., Nano-Met. Chem.* **2005**, *35*, 61–70.
(74) Huang, X.-P.; Spino, M.; Thiessen, J. J. Transport Kinetics of Iron Chelators and Their Chelates in Caco-2 Cells. *Pharm. Res.* **2006**, *23*, 280–290.
(75) Pakchung, A. A. H.; Soe, C. Z.; Codd, R. Studies of Iron-Uptake Mechanisms in Two Bacterial Species of the *Shewanella* Genus Adapted to Middle-Range (*Shewanella putrefaciens*) or Antarctic (*Shewanella gelidimarina*) Temperatures. *Chem. Biodiversity* **2008**, *5*, 2113–2123.
(76) Yamagami, C.; Ogura, T.; Takao, N. Hydrophobicity Parameters Determined by Reversed-phase Liquid Chromatography. *J. Chromatogr.* **1990**, *514*, 123–136.
(77) Richardson, D. R.; Tran, E. H.; Ponka, P. The Potential of Iron Chelators of the Pyridoxal Isonicotinoyl Hydrazone Class as Effective Antiproliferative Agents. *Blood* **1995**, *86*, 4295–4306.
(78) Richardson, D. R.; Ponka, P. The Iron Metabolism of the Human Neuroblastoma Cell: Lack of Relationship Between the Efficacy of Iron Chelation and the Inhibition of DNA Synthesis. *J. Lab. Clin. Med.* **1994**, *124*, 660–671.
(79) Liu, Z. D.; Hider, R. C. Design of Clinically Useful Iron(III)-Selective Chelators. *Med. Res. Rev.* **2001**, *22*, 26–64.
(80) Baker, E.; Richardson, D.; Gross, S.; Ponka, P. Evaluation of the Iron Chelation Potential of Hydrazones of Pyridoxal, Salicylaldehyde and 2-Hydroxy-1-naphthylaldehyde Using the Hepatocyte in Culture. *Hepatology* **1992**, *15*, 492–501.
(81) Richardson, D. R.; Baker, E. Two Saturable Mechanisms of Iron Uptake From Transferrin in Human Melanoma Cells: The Effects of Transferrin Concentration, Chelators, and Metabolic Probes on Transferrin and Iron Uptake. *J. Cell. Physiol.* **1994**, *161*, 160–168.
(82) Mosmann, T. Rapid Colorimetric Assay for Cellular Growth and Survival: Application to Proliferation and Cytotoxicity Assays. *J. Immunol. Methods* **1983**, *65*, 55–63.
(83) Zecca, L.; Youdim, M. B.; Riederer, P.; Connor, J. R.; Crichton, R. R. Iron, Brain Ageing and Neurodegenerative Disorders. *Nat. Rev. Neurochem.* **2004**, *5*, 863–873.
(84) Mabeza, G. F.; Loyevsky, M.; Gordeuk, V. R.; Weiss, G. Iron Chelation Therapy for Malaria: A Review. *Pharmacol. Ther.* **1999**, *81*, 53–75.
(85) Bergeron, R. J.; Weigand, J.; Weimar, W. R.; Vinson, J. R. T.; Bussenius, J.; Yao, G. W.; McManis, J. S. Desazadesmethyldesferrithiocin Analogues as Orally Effective Iron Chelators. *J. Med. Chem.* **1999**, *42*, 95–108.
(86) Parry, S. N.; Ellis, N.; Li, Z.; Maitz, P.; Witting, P. K. Myoglobin Induces Oxidative Stress and Decreases Endocytosis and Monolayer Permissiveness in Cultured Kidney Epithelial Cells without Affecting Viability. *Kidney Blood Press. Res.* **2008**, *31*, 16–28.
(87) Richardson, D. R.; Baker, E. The Uptake of Iron and Transferrin by the Human Malignant Melanoma Cell. *Biochim. Biophys. Acta* **1990**, *1053*, 1–12.
(88) Richardson, D. R.; Baker, E. Intermediate Steps in Cellular Iron Uptake from Transferrin. Detection of a Cytoplasmic Pool of Iron, Free of Transferrin. *J. Biol. Chem.* **1992**, *267*, 21384–21389.
(89) Kalinowski, D. S.; Yu, Y.; Sharpe, P. C.; Islam, M.; Liao, Y.-T.; Lovejoy, D. B.; Kumar, N.; Bernhardt, P. V.; Richardson, D. R. Design, Synthesis, and Characterization of Novel Iron Chelators: Structure−Activity Relationships of the 2-Benzoylpyridine Thiosemicarbazone Series and Their 3-Nitrobenzoyl Analogues as Potent Antitumor Agents. *J. Med. Chem.* **2007**, *50*, 3716–3729.
(90) Richardson, D. R.; Milnes, K. The Potential of Iron Chelators of the Pyridoxal Isonicotinoyl Hydrazone Class as Effective Antiproliferative Agents II: The Mechanism of Action of Ligands Derived from Salicylaldehyde Benzoyl Hydrazone and 2-Hydroxy-1-Naphthylaldehyde Benzoyl Hydrazone. *Blood* **1997**, *89*, 3025–3038.
(91) Yokel, R. A.; Datta, A. K.; Jackson, E. G. Evaluation of Potential Aluminum Chelators in Vitro by Aluminum Solubilization Ability, Aluminum Mobilization from Transferrin and the Octanol/Aqueous Distribution of the Chelators and Their Complexes with Aluminum. *J. Pharmacol. Exp. Ther.* **1991**, *257*, 100–106.
(92) Nick, H. P.; Acklin, P.; Faller, B.; Jin, Y.; Lattman, R.; Rouan, M.-C.; Sergejew, T.; Thomas, H.; Wiegand, H.; Schnebli, H. P. A New, Potent, Orally Active Iron Chelator. In *Iron Chelators: New Development Strategies*; Badman, D. G., Bergeron, R. J., Brittenham, G. M., Eds.; The Saratoga Group: Ponte Vedra Beach, FL, 2000; pp 311−331.
(93) Kotowska, U.; Garbowska, K.; Isidorov, V. A. Distribution Coefficients of Phthalates Between Absorption Fiber and Water and its Use in Quantitative Analysis. *Anal. Chim. Acta* **2006**, *560*, 110–117.